KUOPION YLIOPISTON JULKAISUJA G. - A.I. VIRTANEN -INSTITUUTTI 39
KUOPIO UNIVERSITY PUBLICATIONS G.
A.I. VIRTANEN INSTITUTE FOR MOLECULAR SCIENCES 39

JARNO EELIS MIKKONEN

Short-term Dynamics of Hippocampal Fast Brain Rhythms and Their Implications in the Formation of Functional Neuronal Networks *In Vivo*

Doctoral dissertation

To be presented by permission of the Faculty of Natural and Environmental Sciences of the University of Kuopio for public examination in Auditorium L2, Canthia building, University of Kuopio, on Friday 17th February 2006, at 1 p.m.

Department of Neurobiology
A. I. Virtanen Institute for Molecular Sciences
University of Kuopio

KUOPION YLIOPISTO
KUOPIO 2006

Distributor:
Kuopio University Library
P.O. Box 1627
FI-70211 KUOPIO
FINLAND
Tel. +358 17 163 430
Fax +358 17 163 410
http://www.uku.fi/kirjasto/julkaisutoiminta/julkmyyn.html

Series Editors:
Professor Karl Åkerman, M.D., Ph.D.
Department of Neurobiology
A.I. Virtanen Institute for Molecular Sciences

Research Director Jarmo Wahlfors, Ph.D.
Department of Biotechnology and Molecular Medicine
A.I. Virtanen Institute for Molecular Sciences

Author's address:
Department of Neurobiology
A.I. Virtanen Institute for Molecular Sciences
University of Kuopio
P.O. Box 1627
FI-70211 KUOPIO
FINLAND
Tel. +358 17 163 670
Fax +358 17 163 030

Supervisor:
Research Director, Docent Markku Penttonen, Ph.D.
Department of Neurobiology
A.I. Virtanen Institute for Molecular Sciences

Reviewers:
Docent Stuart Cobb, Ph.D.
Institute of Biomedical and Life Sciences
University of Glasgow
Scotland, UK

Doctor Jozsef Csicsvari, Ph.D.
MRC Anatomical Neuropharmacology Unit
University of Oxford
England, UK

Opponent:
Professor Kai Kaila, Ph.D.
Department of Biological and Environmental Sciences
University of Helsinki

ISBN 951-781-398-8
ISBN 951-27-0422-6 (PDF)
ISSN 1458-7335

Kopijyvä
Kuopio 2006
Finland

Mikkonen, Jarno Eelis. Short-term dynamics of hippocampal fast brain rhythms and their implications in the formation of functional neuronal networks in vivo. Kuopio University Publications G. - A. I. Virtanen Institute for Molecular Sciences 39. 2006. 68 p.

ISBN 951-781-398-8
ISBN 951-27-0422-6 (PDF)
ISSN 1458-7335

Abstract

Rhythmic brain waves are summed extracellular potentials of synchronized neuronal activity. They are ubiquitous in the brain. Interacting neurons form networks that oscillate simultaneously at multiple interleaved frequencies. These frequencies are grouped as bands of frequencies based on their oscillation dynamics. Neurons oscillating at different frequency bands form the brain rhythms which correlate with behavioral states of the organism.

Hippocampus is a medial temporal lobe structure whose neuronal inputs from cortical sensory modalities and outputs to cortex unite in the entorhinal cortex. This specific structure allows detailed exploration of hippocampal brain rhythms revealing principles of neuronal encoding and decoding mechanisms. In this study, I have addressed the role of multiple coinciding fast brain rhythms in hippocampal information transfer and functional network formation. I used electrical stimulations at physiologically relevant numbers and frequencies *in vivo* in Kuopio Wistar rat hippocampus. The extracellular recordings were conducted on 16 channel silicon electrode and a single tungsten wire electrodes, whereas intracellular recordings were performed using sharp capillary glass electrodes. Stimulations had multiple simultaneous frequencies, which mimicked naturally co-occurring brain rhythms of the hippocampus. In our studies, electrical stimuli were targeted intracellularly to single cells in CA3 or extracellularly to fimbria-fornix connecting the CA3 subfields of the hippocampi.

Stimulation of the hippocampal network at gamma, theta and slow frequencies caused repetition of the stimulatory rhythm in subfield CA1 of the hippocampus. The rhythm retained for a time period comparable to short-term memory. Interestingly, stimulation of a single neuron at gamma frequency during hippocampal theta oscillation was sufficient in generating a small-scale CA1 neuronal network oscillating at gamma frequency comparable to the stimulatory gamma frequency. In contrast, combined beta, delta, and slow frequency stimulation was unable to reset the frequency of the CA1 network. However, prolonged beta frequency stimulation induced temporally aligned epileptiform afterdischarges in the whole hippocampus. Our studies demonstrate that oscillation frequencies within hippocampus can be manipulated in order to display memory related patterns. The ability of single neurons to modify and re-organize the existing small-scale neuronal network only at gamma and theta frequencies indicates a mechanism for frequency specific plasticity in brain function. Additionally, stimulations at three distinct frequency bands demonstrated that the frequencies of epileptiform brain rhythms have an inverse relationship: the faster the rhythm the shorter the distance it travels. These results show that brain rhythms, with different frequencies serving different functions, are an active part of information processing and transfer in both normal and epileptiform brain.

National Library of Medicine Classification: WL 102, WL 102.5 WL 150, WL 300, WL 314, WL 335
Medical Subject Headings: brain; hippocampus; temporal lobe; brain mapping; neurons; nerve net; signal transduction; neuronal plasticity; epilepsy; behavior; learning; memory; rats

"Dad and the Work" **Ulla Mikkonen 2001**

Acknowledgements

This work was performed at the A. I. Virtanen Institute, University of Kuopio, during years 1999- 2005.

I wish to express my humble and deepest gratitude to my principal supervisor, Docent Markku Penttonen, Ph.D., Head of the Cognitive Neurobiology Laboratory, for providing me the opportunity and means to fulfill my dream. His enlightenment and sincere enthusiasm on the oscillatory dynamics of the living brain and his faith in my abilities carried me through the moments of disbelief and desperation. I also wish to express my gratefulness to my other supervisors Professor Tapio Grönfors, Ph.D. and Docent Heikki Tanila, M.D., Ph.D. My work would not be complete without Tapio's chaotic conversations and unparallel programming and teaching skills.

I am indebted to Doctor Jozsef Csicsvari and Docent Stuart Cobb, the official reviewers of my dissertation, for their professional and constructive criticism to improve the quality of my manuscript.

I thank Jarno M.A. Tanskanen T.D. for his guidance on the use of Matlab in signal manipulation. I miss the fruitful discussions on the origin of life, species, and the best photograph known to humankind.

I am grateful to Joanna Huttunen M.Sc. for her help and company at the base level of the Institute. May the Force be with you and your growing family.

I thank Jarmo Lappivaara Ph.D. for his never-ending knowledge on physiology and support and guidance and invaluable friendship.

I owe special thanks to the past and the present Cognitive Neurobiology Laboratory staff Sami Kärkkäinen M.Sc., Oleg Ponomarev M.Sc., and Secretary Kaija Pekkarinen.

I thank the neuroscience community of the A. I. Virtanen Institute and University of Kuopio for exuberant and vivid atmosphere and free coffee until 2002.

I am grateful for Matti Vuento and Tuula Jalonen for the opportunity to finish my work and continue my research in the Department of Biological and environmental science at the University of Jyväskylä

I would like to thank AIVI volley for stimulating Wednesday mornings. Additional thanks goes to Jouko Mäkäräinen for letting me enjoy his excellent badminton skills on several other mornings.

I send my warmest thanks to all my friends. Particularly I wish to express my gratitude to Kuopion Uimaseura Waterpoloers for their stimulatory extracurricular activities.

I thank my parents-in law Leena and Risto Kekki for their support.

I do not know how to enough thank my beloved parents and brothers. Mom, Dad, Tommi, Santtu, thank You.

Finally, I dedicate my ultimate love and appreciation to my wife, Anni, for her love, support, and understanding during this process. In addition, special thanks belong to our gremlins Ulla and Lauri. I also thank our late dog Jesse for keeping me fit and in good mental health.

This study was financially supported by the Ministry of Education, the University of Kuopio, the Finnish Cultural Foundation of Northern Savo, the University of Kuopio Fund, the Emil Aaltonen Foundation, and the Ella and Georg Erhnrooth Foundation.

Kuopio, January 2006

Jarno Mikkonen

Abbreviations

ANOVA	analysis of variance
AP	action potential
CA1	cornu Ammonis (Ammon's horn) region 1, a subfield of the hippocampus
CA3	cornu Ammonis region 3, a subfield of the hippocampus
CAP	compound action potential
CSD	current source density
DG	dentate gyrus, a subfield of the hippocampus
EC	entorhinal cortex
EEG	electroencephalography
ES	extracellular stimulation
ff	fimbria-fornix
FIR	finite impulse response
GABA	gamma-aminobutyric acid
IES	combined intracellular and extracellular stimulation
IS	intracellular stimulation
LTD	long-term depression
LTP	long-term potentiation
OLM	oriens-lacunosum moleculare
pp	perforant path(way)
SC	Schaffer collaterals
SLM	stratum lacunosum moleculare
SO	stratum oriens
SP	stratum pyramidale
SR	stratum radiatum
SUB	subiculum
UFO	ultra-fast oscillation

Publications

Mikkonen J.E., Huttunen J., and Penttonen M. (2006) Contribution of a single CA3 neuron to network synchrony; *NeuroImage* ***(in press)***

Mikkonen J.E., Penttonen M. (2005) Frequency bands and spatiotemporal dynamics of beta burst stimulation induced afterdischarges in rat hippocampus *in vivo*; *Neuroscience* ***130****, 239-247*

Mikkonen J.E., Grönfors T., Chrobak J.J. and Penttonen M. (2002) Hippocampus retains the periodicity of gamma stimulation *in vivo*; *Journal of Neurophysiology* ***88****, 2349-2354*

Table of contents

Chapter 1
General introduction

Rhythmic brain waves have been recorded from mammalian brain since 1875 (Caton 1875). Merriam Webster dictionary defines brain waves as "rhythmic fluctuations of voltage between parts of the brain resulting in the flow of an electric current" (Merriam-Webster online dictionary 2006). Recording of these oscillatory rhythms is actually a recording of the potential difference between two conducting metal wires called electrodes. The commonly used term electroencephalography (EEG) denotes recording, *graph*, of electrical signals, *electro*, from the brain, *encephalon*. This term refers to recordings from the surface of the brain outside the skull. When electrodes are inserted into the brain and potential differences are recorded outside the cells, or extracellularly, the equivalent term is local field potential or deep EEG. Local field potential recording sums the potential differences generated by all the neurons near the electrodes. Sometimes, a term compound action potential is also used in order to emphasize that a sum of action potentials of individual neurons is recorded. Intracellular recordings of single cells yield pure action potentials. Electrophysiology is the study of intracellular membrane potentials, action potentials, and local field potentials in relation to the function of the nervous system. The brain rhythms stem from both internal and external factors (Fellous and Sejnowski 2000). The former factors are the intrinsic membrane properties of each neuron, the composition of ion channels and transmembrane proteins on the plasma membrane surface and their function. The latter factors influencing rhythms, more related to this dissertation, are the connections of each neuron, the inputs neuron receives.

Information encoding and transfer in the brain have been classically divided into two competing interpretations of the trains of action potentials. One claims that the brain "code" is based on the rate of firing of the working neurons (rate code). The other states that the temporal difference between spikes is important (temporal code). Then there are the rhythmic brain waves. Irrespective of the code, neurons form dynamic networks that operate at multiple different frequencies thus comprising a mosaic of oscillators within the brain. Furthermore, the different oscillation frequencies have been correlated to specific functional stages of an animal and, therefore, are most likely connected to the cognitive neuronal network functions (Phillips and Singer 1997). In fact, Lisman and Idiart (1995), and Jensen and Lisman (2005) have proposed that oscillation subcycles could be the timing mechanism to control the processing of short-term memories. Building on top of the Hebbian view (1949), this approach predicts that information is packed on multiple levels of individual signals involving brain rhythms at different frequencies and both rate and temporal codes of the action potential trains. This approach would diminish the number of neurons needed to process each piece of information, and consequently, would increase the efficiency of neuronal networks. However, little is known about how individual neurons interact to create the observed synchronous neuronal ensembles or small-scale networks in the brain (Cavazos et al. 1994; MacLeod et al. 1998). This dissertation focuses on the frequency and temporal principles of functional small-scale neuronal network formation *in vivo*.

1.1 Hippocampus

Hippocampus is probably the most studied structure in the brain. It is located in the medial temporal lobe where its main pathway forms a unidirectional, tri-synaptic loop from entorhinal cortex to entorhinal cortex. Additionally, the hippocampus is tightly packed into distinct cellular layers of excitatory principal cells thus making the structure easy to explore. Furthermore, the loop feature of the hippocampal pathway uniquely binds hippocampus into information refinement and storage (O'Keefe and Nadel 1978). Previous studies have shown that hippocampal oscillations play a significant role in learning and memory functions (Buzsaki 1989; O'Keefe and Recce 1993; Lisman and Idiart 1995; Kolta et al. 1996).

1.1.1 Hippocampal anatomy and physiology in brief

Majority of the hippocampal anatomy was revealed over a hundred years ago by Ramon y Cajal (DeFelipe and Jones 1992). As a functional refinement to mere anatomy, current source density analysis based on local field potentials emerged during the 1970's (Freeman and Nicholson 1975). The modern view of hippocampus has been illustrated by Amaral and Witter (1995). Hippocampus proper consists of Ammon's horn or cornu Ammonis regions 1-3 whereas hippocampal formation involves also dentate gyrus (DG), subiculum and entorhinal cortex (Figure 1.1). Information from neocortical sensory modalities enters hippocampus *via* perforant pathway, which originates in the superficial layers of the entorhinal cortex and terminates in DG. DG is rich with inhibitory interneurons and acts as a gate into the hippocampus proper. It is the discriminator of the incoming information (Buzsaki and Freund 1996). DG connects to cornu Ammonis region 3 (CA3) along mossy fibers. Next, CA3 connects to cornu Ammonis region 1 (CA1) through Schaffer collaterals and, finally, the information escapes hippocampus from CA1 to subiculum and the deep layers of the entorhinal cortex. Actually, the Ammon's horn is divided into four segments, CA1 through CA4, but for the purpose of this dissertation the functionally relevant subfields (Bernard and Wheal 1994) are the largest ones: CA3 and CA1. Therefore, in this dissertation a simplified description of hippocampus is used, involving only DG, CA3 and CA1.

Hippocampal dendrites have differing morphology and function at apical and basal portions across different subfields (Freeman and Nicholson 1975; DeFelipe and Jones 1992; Kloosterman et al. 2001). CA3 receives input from excitatory granule cells of the dentate gyrus. CA3 has been named as the auto-associative part of the hippocampus due to its richness in recurrent collaterals between the excitatory principal cells (Miles and Wong 1986). In contrast, CA1 somatic recurrent collaterals are very rare. However, CA1 basal dendrites have interconnections (Kaibara and Leung 1993), and, most importantly, CA1 principal cells are connected *via* electrical synapses (Connors and Long 2004). The CA1 receives CA3 inputs mainly *via* the synapses at the junction of CA3 principal cells axons and the middle portion of the CA1 apical dendrites, the Schaffer collaterals. This middle portion of the CA1 apical dendrites is called *stratum radiatum*. Additionally, there are synaptic connections directly from the entorhinal cortex that terminate at the distal portion of the apical dendrites at *stratum lacunosum moleculare* of CA3 and CA1. Basal CA1 dendrites at the *stratum oriens* receive input from the CA3 and from CA1 collaterals. In addition to these

main excitatory connections, the inhibitory interneurons connect subfield and region specifically to destined parts of the principal cell dendrites, axons or soma. Some of these interneurons target other interneurons providing the hippocampus with another barrage of ways to organize and reorganize the connections, thus further complicating the anatomical and physiological connections within hippocampus.

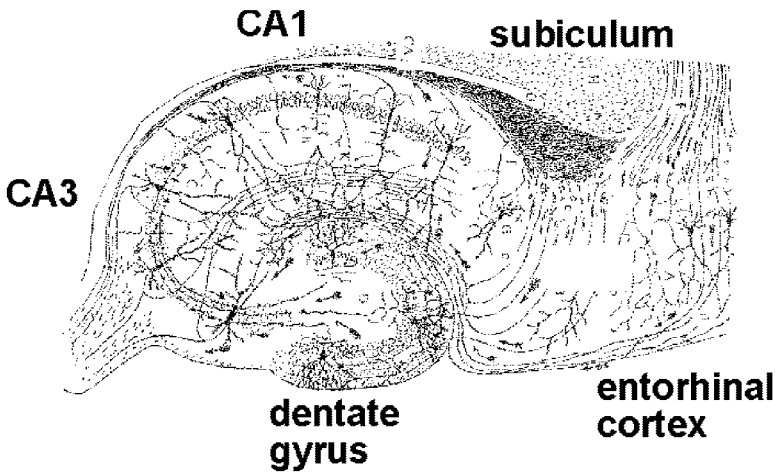

Figure 1.1. Hippocampus. Figure modified after Ramon Y Cajal's famous drawing. Figure demonstrates the loop like structure of the hippocampus starting from the entorhinal cortex and returning to the entorhinal cortex. Note also the densely packed principal cell subfields dentate gyrus, CA3 and CA1.

There are fiber tracts connecting the two hippocampi on either side of the brain: the dorsal and the ventral hippocampal commissures (Amaral and Witter 1989). The ventral hippocampal commissure consists of fibers running in the fimbria and turning back at the rostral end of the hippocampus to run in the fimbria of the other hemisphere (O'Keefe and Nadel 1978). Additionally, over 30 subcortical structures connect to hippocampus (Swanson 1977; Buzsaki et al. 1989), from which the most prominent structures are medial septum and Raphe nucleus (Swanson 1977; Freund et al. 1990; Gulyas et al. 1999). Entorhinal cortex connects directly to all hippocampal regions (O'Keefe and Nadel 1978; Amaral and Witter 1989).

Medial septal neurons are important for hippocampal neuronal network. The inhibitory GABAergic projections from septum terminate on hippocampal interneurons (Stewart and Fox 1990; Dragoi et al.1999). These projections are important for pacing the hippocampal theta rhythm described in chapter 1.2.1. Additionally, the cholinergic neurons of the medial septum connect to all regions of the hippocampus proper and modulate the responsiveness of their hippocampal target neurons (Hasselmo and Schnell 1994; Hasselmo et al. 1995; Hyman et al. 2003).

1.1.2 Basic neuronal types in hippocampus

Principal cell subfields of hippocampus proper are illustrated in the figure 1.1. Each of the hippocampal subfields is tightly packed with excitatory principal neurons. Dentate principal neurons are called granule cells, whereas CA3 and CA1 principal cells are called pyramidal cells. Up to ninety percent of the hippocampal neurons are excitatory principal neurons. These principal neurons are surrounded by a stream of different inhibitory interneurons. Although different interneurons can be identified immunohistochemically based on the presence of different calcium binding proteins (e.g. calbindin, calretinin, and parvalbumin) in the cells, the purpose of different interneurons is not fully understood. Nevertheless, Freund and Buzsaki (1996), and Somogyi and Klausberger (2005) have classified the hippocampal interneurons depending on their location and morphology in relation to the principal cell subfields. Most important CA1 interneurons, basket cells, bistratified cells, chandelier cells, and oriens-lacunosum moleculare (OLM) cells, are schematically illustrated in figure 1.2. Interneuronal projections have an internal order that optimally suppresses and controls principal cell firing. Furthermore, a division of labor seems to exist whereby different frequencies and spatiotemporal properties of hippocampal rhythms are controlled by different types of interneurons (Gloveli et al. 2005).

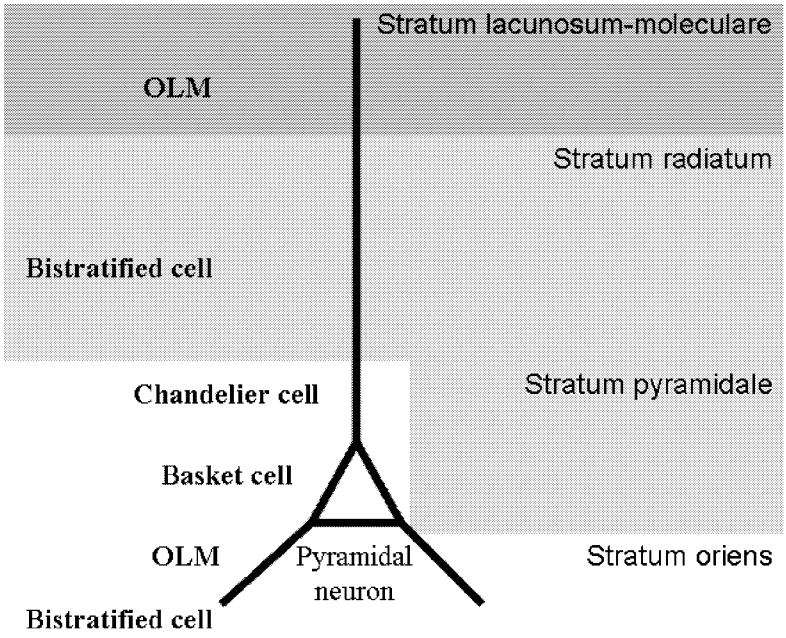

Figure 1.2. Hippocampal CA1 pyramidal cell and its interneurons. CA1 pyramidal neuron is schematically illustrated in the middle. Different subfields (strata) around the cell are illustrated on the right side of the cell and also with different intensities of gray. On the left side of the cell different interneurons are labeled on their synaptic target layers. Note that the bistratified cell and the OLM cell have target synapses on two layers.

Basket cells innervate soma and proximal dendrites whereas chandelier cells target action potential initiation segments of the principal cells in an attempt to silence the whole neurons. This is the basis of the common model on how gamma rhythm is generated in the hippocampus. This model states that the above mentioned interneurons are ideally positioned to force the principal cells into synchronous firing. Because their cell soma is smaller and their kinetics different (Fricker and Miles 2000), they reach the firing threshold faster than the principal cells. Thereafter, they suppress the principal cells and inhibit them from firing action potentials. Each interneuron connects to hundreds of principal cells. Thereby, all these principal cells recover from interneuron induced inhibition at approximately the same time, and as a rebound to the inhibition (Jefferys et al. 1996; Wang and Buzsaki 1996), they fire. The firing triggers again basket and chandelier cells, which suppress the principal cells and the cycle starts again. This way, the soma targeting interneurons generate synchronous populations of principal cells. These synchronous population activities are the ones that are recorded as hippocampal brain rhythms.

Interneurons called the bistratified cells have axons that omit the principal cell soma, but target the apical and basal dendrites of the principal cell layers. In *stratum radiatum* bistratified cells target CA1 dendrites at the same site where CA3 axons, the Schaffer collaterals, connect to the CA1 dendrites. Their axons do not spread over many principal cells but rather specifically block certain branches of the principal cell dendritic tree (Freund and Buzsaki 1996). This way bistratified cells are not as total in blocking the firing of the whole principal cell as basket and chandelier cells, but they can subtly modify or direct the output of the principal cell network. Contrary, the OLM cells are excited by the basal dendrites of the CA1 principal cells, the *stratum oriens* and inhibit the very distal portion of the apical dendrites in the *stratum lacunosum moleculare*, where the axons from the entorhinal cortex directly contact CA1 principal cell dendrites (Freund and Buzsaki 1996; Wu and Leung 2003). Thus, the OLM cell has a crucial role in permitting or inhibiting direct entorhinal signaling to CA1.

1.1.3 Normal and abnormal function of hippocampus

The importance of hippocampus in memory became evident in the 1950's when bilateral removal of hippocampus in one epilepsy patient led to devastating memory loss (Scoville and Milner 1957). This has been confirmed later by neuropsychological examination of patients with damage to the medial temporal lobe and by experimental lesion studies in rodents (Eichenbaum 2000).

Whereas neuropsychological studies on human patients have emphasized the role of hippocampus in episodic memory (Squire and Zola-Morgan 1991) studies in rodents found hippocampus to be specialized in spatial navigation and memory (Morris et al. 1982). Further evidence for the special role of hippocampus in spatial processing came with the finding of place cells. O'Keefe and Nadel (1978) summed the hippocampus as a cognitive map: hippocampus forms an internal representation of the environment. This representation is realized in the firing of a group of hippocampal principal cells coding for that space. These

place cells fire only at a specific location in the environment. By summing the activity of place cells hippocampus forms representations known as place fields, which can be considered as coded maps of the given environment. Moreover, these place fields remap in new environment while retaining the old map configuration (Muller and Kubie 1987).

The above mentioned views are not mutually exclusive, however, as hippocampal activation has been reported in human during a mental navigation task (Maguire et al. 1997) and hippocampal lesions in rodents lead to impairment in episodic like memory tasks (Eichenbaum 2000).

Hippocampal oscillations not only code for learning and memory. Hippocampus displays also pathological oscillations, such as occur during epilepsy. Indeed, temporal lobe epilepsy is the most common type of adult onset epilepsy. The epilepsy often begins in hippocampus, where it damages inhibitory interneurons at hilar regions surrounding the dentate gyrus (Lowenstein et al. 1992). In functional terms, uncontrolled simultaneous firing of networks of neurons is characteristic to epilepsy (McCormick and Contreras 2001). The anatomical hallmark of hippocampal epilepsy is cell loss at the above mentioned hilar regions and a subsequent atrophy of the CA1 (Babb and Brown 1987) and sprouting of recurrent excitatory collaterals by granule cell axons (Golarai et al. 2001).

1.2 Plasticity, spike timing, and frequencies

One important aspect of frequency dependent information transfer in the hippocampus and brain in general is plasticity. Plasticity refers to continuous activity-dependent modification of synaptic efficacy. The most commonly referred terms of plasticity are long-term potentiation (LTP) and long-term depression (LTD). Sometimes LTD is further divided into depotentiation and actual depression. Here LTD covers both terms, unless otherwise stated. LTP and LTD are the most studied forms of Hebbian (1949) synaptic plasticity (Heynen and Bear 2001). They are defined as long lasting increase (LTP) or decrease (LTD) in synaptic transmission efficacy and are believed to play a crucial role in learning and memory (Contreras et al. 1996). One interpretation of LTD is that the firing rate of the affected local ensembles of neurons is suppressed by interneurons, and therefore, an oscillating environment for the larger neuron ensembles may be created (Traub et al. 1985). Also the specific roles of LTP, although linked with memory functions, remain unsolved (Holscher et al. 1997a). In electrophysiological studies, LTP in hippocampal CA1 can be generated with continuous high frequency stimulation or patterned burst stimulation (Evans et al. 1994). Furthermore, Holscher et al. (1997b) have shown that LTP can be induced with a single burst (5 pulses at 200 Hz) at the positive phase of theta activity. Additionally, a similar pulse on the negative phase did depotentiate the studied cells, but did not cause depression. However, Hyman et al. (2003) demonstrated that stimulation to the peak of theta caused LTP and stimulation to the trough caused LTD in the CA1 of behaving rats. Since the hippocampus switches to theta phase when the animal enters a new environment, theta has been defined as an exploratory oscillation phase (Zador et al. 1990). Association of theta and LTP, on the other hand, strongly suggests that there must be a link between the two and memory formation (Tsodyks

et al. 1996). On the other hand, Gray (1994) discovered that LTP can be induced when synaptic input and neuronal firing occur nearly simultaneously within the range of gamma oscillation, and synaptic input precedes cellular discharge by about 10 ms, and LTD in the reversed order. In the light of the recent experiments, it would be crucial to investigate the role of different oscillation frequencies in relation to network behavior.

In the network sense plasticity promotes formation of transient functional networks or ensembles of neurons. Computer-like hard wired system would be too rigorous and thereby would limit the information transfer that is required for efficient brain function. Due to the fact that incoming sensory information requires immediate responses and adaptation, the underlying neuronal architecture must have flexible relations. Hebb (1949) proposed that individual neurons represent only general and simple features. The presence of the whole environment is then signaled by the simultaneous responses of groups of neurons, each responding to their respective components. Now the same neuron acts upon different objects or components of the environment at different times and, subsequently, forms different neuronal groups with other neurons. Thus there would be no strict paths of information flow in the brain but the signal could belong to any number of neuronal paths or groups that code for the specific occurrence in the environment. This would enhance neuronal network capacity to form associative networks. Such re-use of connections and re-organization of the structure could occur if the brain used oscillations as a network code.

1.2.1 Division of hippocampal brain rhythms by frequency

Traditionally, brain rhythms have been arbitrarily divided into frequency bands corresponding to the observed physiological human or animal data. We have an inconstant naming of the frequency bands where recently discovered low and high bands have descriptive nomenclature and the older middle bands have Greek alphabets. The rhythms present in hippocampus are divided into following bands (Penttonen and Buzsaki 2003):

- slow (4) 0.02-0.06 Hz
- slow (3) 0.06-0.2 Hz
- slow (2) 0.2-0.5 Hz
- slow (1) 0.5-1.5 Hz
- delta (δ) 1.5-4 Hz
- theta (θ) 4-10 Hz
- beta (β, spindle) 10-30 Hz
- gamma (γ) 30-80 Hz
- fast 80-200 Hz
- ultra-fast 200-600 Hz

It is noteworthy that these frequency ranges of frequency bands are not fixed, but vary depending on the experiment, species and anesthetic. In this dissertation gamma band limits 20-70 Hz, 20-80 Hz, 25-75 Hz, and 30-80 Hz are interchangeably used. Similarly beta band limits 8-20 Hz, 8-30 Hz, 8-25 Hz, 10-25 Hz, and 10-30 Hz are used.

One of the highest frequencies recorded from hippocampus to date are ultra-fast oscillations or UFOs described by Bragin et al. (2002). These oscillations are multiunit oscillations involving a network where neighboring neurons generate the observed high rhythm. UFOs usually relate to epileptic conditions. Next frequency bands in succession, the fast, gamma, beta, theta, and delta bands, have been the most studied frequency ranges in the brain. Occasionally beta band is split in two, alpha (10-20 Hz) and beta (20-30 Hz) bands. These bands go also by the names beta I and beta II, respectively. Additionally, Contreras and Steriade (1995) have discovered a functional subtype of beta band called the spindle. Originally this referred to 14 Hz thalamic sleep spindles, but has now been widely used also for other brain regions displaying similar behavior. The theta rhythm plays a role in the representation of spatial information (O'Keefe and Recce 1993; Skaggs et al. 1996; Kahana et al. 1999) and facilitates the induction of synaptic plasticity (Buzsaki 1989; Huerta and Lisman 1993). Despite the fact that these frequency bands form a linear succession in natural logarithmic scale (Penttonen and Buzsaki 2003) very little investigations have been conducted to study the interrelationships between more than two frequency bands.

This dissertation tries to overcome the rapid temporal variations and stochastic changes occurring in the brain in frequency-domain analyses. Interpretation and analysis of brain rhythms is affected by the properties of amplifiers. Early electrophysiological research used high gain alternating current amplifiers to achieve the necessary amplification to observe the low amplitude rhythmicity from the scalp. This amplifier provided a method for filtering slow periodic and non-periodic influences and allowed the observation and quantification of low amplitude oscillations characteristic of the EEG. Contemporary amplifiers provide higher gain and greater stability, but the basic methods in electrophysiology have changed little over the past 50 years. Usually, the same input signal is used for both evoked potential and EEG research. However, evoked potential research emphasizes the low frequency influence of the voltage shifts associated with stimulus processing by expanding the low frequencies passed by the amplifier *via* longer time constants. In contrast, EEG research emphasizes the high frequency content by attenuating the low frequency activity *via* short time constants. Additionally, the periodicity, or the rhythmicity of the oscillating neurons is not sinusoidal, but varies in an unexpected manner. Thereby, averaging or automatic filtering often yields distorted characteristics of the signals of interest: the interesting short-term frequency changes of the non-stationary brain signal are filtered out. Therefore, this dissertation benefits from a broad-band approach (high-pass filtering at 0.1 Hz and low-pass filtering at 6 kHz) followed by applied time-frequency analysis and sophisticated statistical measures aiming at preserving the interesting short-term deflections in the brain signal with minimal averaging.

1.2.2 Division of hippocampal brain rhythms by function

Hippocampal rhythms are behavioral state dependent. In other words, there is a contemporaneous division between different patterns of behavioral activity and neuronal activity. During exploration, navigation, memory tasks, learning, and rapid eye movement sleep brain operates at least at *gamma*, *theta*, and *slow* frequencies (Buzsaki 1989; O'Keefe

and Recce 1993; Fellous and Sejnowski 2000). In contrast, *fast*, *beta*, and *delta* frequencies coincide with apparently passive behavior, consummation, or merely internal activities (Buzsaki 1989; Bragin et al. 1997; Sirota et al. 2003). In addition to behavior, division of labor exists between different frequencies being controlled by different interneurons (Gloveli et al. 2005). As mentioned previously, OLM cells are likely to provide output to distal dendritic segments. This effect seems to be theta-frequency patterned (Buzsaki 2002). Basket and bistratified cells are involved in the generation of locally synchronous gamma band oscillations.

Gamma (Buzsaki et al. 1983; Soltesz and Deschenes 1993; Bragin et al. 1995) and theta (Green and Arduni 1954; Vanderwolf 1969; Bland 1986; Stewart and Fox 1990) frequencies have been reported to coincide with information acquisition and processing in hippocampus (Lisman and Idiart 1995; Chrobak and Buzsaki 1998a; Jensen and Lisman 2005). Additionally, the same frequency bands have been shown to be active at the spatial mapping and firing of the place cells. Lisman and Idiart (1995) have suggested that gamma and theta frequency cycles could be used for storage of short-term memories. Interestingly, the neurons that fire at gamma and theta frequencies during awaken exploration fire in exactly the same order during sleep, albeit at higher frequencies (Draguhn et al. 2000; Pennartz et al. 2004). This fast-forward type of activation of the awake networks during subsequent sleep might indicate how brain processes information at different frequency networks, especially if these networks were more or less mutually exclusive.

1.2.3 Network dynamics at different frequencies

Transient hippocampal fast frequencies are generated in local neuronal ensembles (Bragin et al. 2002). Gamma frequencies, on the other hand, require larger ensembles with inhibitory interneuron interactions (Wang and Buzsaki 1996). In contrast, hippocampal beta frequencies require ensembles with intrahippocampal pyramidal cell oscillators (Jefferys 2003). Theta frequencies emerge from interplay between various structures including hippocampus proper, medial septum and raphe nucleus (Freund et al. 1990; Dragoi et al. 1999). Slower rhythms seem to include larger brain areas for activation (Penttonen and Buzsaki 2003). For example, hippocampal delta frequencies are initiated both in entorhinal cortex and hippocampus (Pare et al. 1992; Barbarosie and Avoli 1997).

Gloveli et al. (1997), Henze et al. (2002), and Mori et al. (2004) have reported frequency dependent information transfer within the nervous system. This is not just summation of the inputs, where individual input responses build up and eventually trigger the cell to fire. In frequency dependent information transfer, also the intrinsic properties of the neurons and the organization of the neuronal network favor transmission at certain frequencies. Typically the reported frequencies have been around theta range for large networks and above beta (>20 Hz) for smaller networks (Steriade 1998; Fellous and Sejnowski 2000; Penttonen and Buzsaki 2003; Sirota et al. 2003). However, little experimental information is available on functional network dynamics at multiple coexisting frequency bands.

1.3 Objectives

The aim of this dissertation is to reveal and explain frequency specific mechanisms underlying origination and co-operability in functional neuronal networks and how they may contribute to synaptic plasticity, and subsequently memory formation in the hippocampus. Especially, the coherent activity of neuronal ensembles during behaviorally relevant synchronous population events in the hippocampus is discussed. This dissertation aims at providing novel and unifying insight on different forms of temporally coordinated oscillatory activities in the hippocampus and their contribution to formation of functional neuronal networks.

This dissertation focuses on the role of intracellular single cell and extracellular field oscillations of the hippocampus in the functional neuronal network formation. In particular, the CA3-CA1 hippocampal neuronal network is studied using intracellular and extracellular recordings to different stimulation patterns to discover alterations in the network dynamics and subsequently in the neuronal cooperation. This study evaluates the ability of induced *in vivo* resembling oscillations to generate temporary oscillatory networks in the hippocampus.

The questions this dissertation engages to unravel are as follows:

1. *can specific frequencies be repeated in hippocampal neuronal network,*
2. *how do the frequencies correlate with network size, and*
3. *how does the interaction between a neuron and a network occur.*

Moreover, the specific aims of this dissertation are:

1. *to describe the possible frequency preferences of hippocampal neurons and the effects of those frequencies in network oscillations,*
2. *to manipulate the oscillation frequencies within hippocampus in order to display memory related patterns, and*
3. *to demonstrate the functional relationship between oscillations in single cells and networks within hippocampus.*

In conclusion, this dissertation quests mechanisms underlying hippocampal cell assembly formation and examines the basis of rhythmicity underlying cooperative activity between hippocampal neurons and neuronal networks *in vivo*.

1.4 Outline of the dissertation

Although the fundamental properties of neurons are well known, the synergistic nature of neuronal networks and the communication between neurons and networks is still all but clear (Kohling et al. 1999). In hippocampus, synchronous gamma and theta oscillations have been shown to coexist in the network (Bragin et al. 1995; Lisman and Idiart 1995; Buzsaki 2002). The synchronization reflects the underlying interneuronal network, which oscillates at gamma and theta frequencies and controls the firing of the principal cells (Wang and Buzsaki 1996). This synchronous oscillation, however, does not fully describe the network. Henze et al. (2002) demonstrated that the connection between dentate gyrus and CA3 depends on firing

frequency and repetition. Nevertheless, the close relationship between a neuron's position, connections, and firing frequency in the network should be further examined. This dissertation concentrates on recognizing the relationships between different frequencies in CA3-CA1 neuronal network and its individual neurons, and hypothesizes on the behavior that is governed by that network, forming a double-stranded explanation of structure and function.

Chapter 2 describes how frequency specific information can be formed and retained in the hippocampal neuronal network. This requires copying the oscillatory structure of the hippocampus and, especially, mimicking its frequencies. Extracellular fimbria-fornix stimulations that are *in vivo* patterned are used in order to resemble naturally co-occurring gamma and theta oscillations. Then intra- and extracellular recordings from CA1 area demonstrate that at least the small-scale network visible to recording electrodes is entrained by the patterned stimulation and repeats the artificial rhythm evoked by the stimulation. The entrainment and retention of the rhythm support the previous works by Lisman and Idiart (1995), and Jensen and Lisman (2005) on the oscillatory short-term memory formation in the hippocampus.

The frequency preferences of the hippocampal neuronal networks are further discussed in Chapter 3. This chapter demonstrates that repetition of a combined stimulation of beta, delta, and slow frequencies drives the hippocampus into an epileptiform state of uncontrolled firing of large groups of neurons at all cellular subfields of the hippocampus. This uncontrolled bursting, however, has an internal structure that allowed interpretation of the organization of the formed bursting oscillators. The observed afterdischarge bursts occurred at fast, beta, and delta frequencies. From these frequency bands, fast frequencies correlated only with their neighbors, whereas beta frequencies correlated also between hippocampal subfields and delta frequencies correlated across the recorded hippocampus. In other words, high frequencies connect local and low frequencies distant neurons into networks.

Chapter 4 returns to hippocampal gamma frequencies, but with a different perspective. This chapter describes how single neurons can act as founders for functional neuronal networks. This chapter sums the previous chapters in a fundamental sense since it describes how the events described in chapters 2 and 3 can ever occur. Any single CA3 pyramidal cell oscillating at gamma frequency can, at a favorable network state, act as a pacemaker who transfers its rhythm to its neighbors and eventually into an ensemble of neurons in the successive cellular subfield. One cell can drive an ensemble of cells.

The concluding remarks (Chapter 5) briefly discuss the main findings of this dissertation and review the novel aspects arisen on the basis of the findings. In this final chapter I illuminate this dissertation as an entity that will explain the necessity of exploration of the brain in the frequency domain.

Chapter 2
Hippocampus retains the periodicity of gamma stimulation *in vivo*

Several behavioral state dependent oscillatory rhythms have been identified in the brain. Of these neuronal rhythms, gamma (20-70 Hz) oscillations are prominent in the activated brain and are associated with various behavioral functions ranging from sensory binding to memory. Hippocampal gamma oscillations represent a widely studied band of frequencies co-occurring with information acquisition. However, induction of specific gamma frequencies within the hippocampal neuronal network has not been satisfactorily established. Using both *in vivo* intracellular and extracellular recordings from anesthetized rats, we show that hippocampal CA1 pyramidal cells can discharge at frequencies determined by the preceding gamma stimulation, provided that the gamma is introduced in theta cycles, as occurs *in vivo*. The dynamic short-term alterations in the oscillatory discharge described in this paper may serve as a coding mechanism in cortical neuronal networks.

2.1 Introduction

Hippocampus exhibits two distinct operational states defined by specific oscillatory rhythms. The "unaroused" hippocampus exhibits bursts of high frequency (70-200 Hz) ripples interspaced by lower beta (12-20 Hz) and delta (1-3 Hz) frequency rhythms, whereas the "aroused" hippocampus exhibits gamma (20-70 Hz) frequencies nesting within the theta (3-12 Hz) rhythm (Bragin et al. 1995; Traub et al. 1996; Chrobak and Buzsaki 1998b). Theta-modulated gamma occurs during periods of focused attention, exploratory movement, and rapid-eye movement sleep, thus coinciding with flow of sensory-dependent patterns of neural activity into the hippocampus from the neocortex. Thus, it is likely that theta-modulated gamma relates to a period of "information acquisition" within hippocampal circuits (Chrobak and Buzsaki 1998a).

Hippocampal gamma oscillations reflect the underlying intrinsic interneuronal network rhythm of interneuron-interneuron connections, which are stabilized by excitatory connections (Whittington et al. 2000). The interneuronal network gamma oscillation appears to create and coordinate time windows for synchronized firing within networks of pyramidal cells (Buzsaki and Chrobak 1995; Penttonen et al. 1998; Whittington et al. 2000). Although gamma frequency time frames (14-50 ms) have been linked to hippocampal loop times (Pare and Llinas 1995) and delay lines (Bi and Poo 1998), the presence of prominent gamma oscillations in hippocampal slices (Whittington et al. 1997; Doheny et al. 2000) and in local hippocampal ensembles *in vivo* suggest that at least part of the gamma oscillation is generated *in situ*. Pyramidal cell membrane depolarization levels (Penttonen et al. 1998), time constants (Volgushev et al. 1998), and ephaptic field effects (Bracci et al. 1999; Whittington et al. 2001), have been proposed as local generators of gamma oscillations at various frequencies. In addition, the frequency of the interneuronal network gamma oscillations has been shown to depend on $GABA_A$ decay time constants (Whittington et al. 1995; Wang and Buzsaki 1996; Olypher 1998; Traub et al. 1998). In the present work, we recorded, both extracellularly and

intracellularly, rat CA1 pyramidal neurons *in vivo,* and examined their response to contralateral fimbria-fornix stimulation at natural gamma nested theta frequency patterns. Our results show that CA1 pyramidal cells can retain the gamma pattern induced by gamma/theta - patterned fimbria-fornix stimulation.

2.2 Methods

2.2.1 *In vivo* methodology

Experiments were conducted on 25 Kuopio Wistar rats (250-350 g) anesthetized with 1.1-1.4 g/kg urethane. The methods used in the experiments have been approved by the State Provincial Office of Eastern Finland (approval number 99-61). The animal was placed in a stereotaxic instrument (Kopf series 962), the scalp was removed, and small bone windows were drilled above the target structures (Fig. 2.1). A pair of stainless steel wires (100 μm in diameter) with 0.2-0.4 mm tip separation was placed in the fimbria-fornix (-1.3 mm anteroposterior from bregma; +1.0 mm lateral from midline; -4.0 mm ventral from cortical brain surface) to stimulate commissural afferents to the contralateral CA3 region. The intensity of the 0.2 ms electrical pulse stimulation (Master8 pulse generator and Iso-flex stimulus isolator, A.M.P.I, Jerusalem, Israel) was twice the threshold capable of inducing compound action potentials (CAPs) in more than two consecutive trials. The stimulation intensity was between 140 and 300 μA. In six experiments, higher stimulation intensities (3 and 4 times the threshold) were tested in order to determine the possible intensity-related alterations in induced CAP frequencies. Micropipettes for intracellular recordings (resistance 80-120 MΩ) were pulled from 1mm filamented quartz capillary glass (P2000 Sutter Instruments, Novato, CA, USA) and filled with 3 M potassium acetate, whereas single tungsten wire (60 μm in diameter) was used for extracellular field potential recordings. Vertical positioning to the CA1 pyramidal layer for the extracellular (25 animals; -3.6 mm anteroposterior from bregma; -4.0 mm lateral from midline at 30° angle) and intracellular (5 animals; -3.6 mm anteroposterior from bregma; -2.2 mm lateral from midline) recording electrodes were estimated from the polarity of the field response, the shape and firing patterns of the CAPs and action potentials (APs), and from the latency of the evoked field response (7-12 ms). The pathway of the stimulation (fimbria-fornix - CA3 - CA1) was confirmed by lowering the recording electrode into the CA3 area of the hippocampus to record antidromic CAPs with a latency of 3-5 ms to the stimulation. Typically the CA1 pyramidal layer was located -2.0 ± 0.1 mm below the cortical surface. Two stainless steel watch screws, driven into the bone above the cerebellum served as indifferent and ground electrodes in the extracellular recordings, whereas a single subcutaneous chlorinated silver wire was used as the indifferent electrode for intracellular recordings.

2.2.2 Stimulations and recordings

We constructed an *in vivo* pattern -resembling stimulation protocol using naturally co-occurring gamma and theta frequencies (Fig. 2.1). There is considerable variance in the frequency range definitions of different frequency bands in the literature. In our experiment, we selected the frequency band values that, in our opinion, most accurately describe the representative frequency bands decelerated by urethane anesthesia (Ylinen et al. 1995a;

Penttonen et al. 1998). Each stimulation epoch had a total of 64 pulses that were spaced so that four gamma pulses (30-60 Hz) were embedded in a theta cycle that was repeated 4 times at 3-7.5 Hz frequencies. This 16 pulse gamma/theta -pattern was then repeated a maximum of four times at 0.3-0.5 Hz (see Figs. 2.1 and 2.3). In an individual stimulation epoch, gamma and theta frequencies were kept constant. The stimulation frequencies were varied across stimulation epochs so that that each animal received at least three different gamma frequencies, and each of them twice, from lower to higher to lower frequency (e.g. 30 Hz- 40 Hz- 50 Hz- 40 Hz- 30 Hz) or *vice versa* (50 Hz- 40 Hz- 30 Hz- 40 Hz- 50 Hz). Stimulation theta frequency was constant during such gamma frequency manipulation. The stimulation epochs were repeated at 3-10 minute intervals for one hour, after which the animal was left unstimulated for 30 to 60 minutes. Each animal experienced 2-3 one-hour stimulation sessions. The final recordings from 10 animals involved prolonged 10-20 s stimulations with an increased number of stimulation pulses. These stimulations had an increased number of cycles (6-8) in one or more of the stimulation time frames, or used a reduced protocol with only 3-5 second gamma stimulations or 5-10 second theta modulated gamma stimulations. The intracellular signal was tenfold amplified using an Axoclamp 2B amplifier (Axon Instruments, Foster City, CA, USA), then further fourfold amplified with a Cyberamp380 (Axon Instruments). The EEG signal was 1000-fold amplified using a custom-made amplifier. Thereafter, both signals were low-pass filtered at 6 kHz (Cyberamp380, Axon Instruments), and finally sampled with 16-bit precision at 10 kHz (Digidata 1320A; Axon Instruments). The data were stored on a computer hard disk using Axoscope 8.0 data acquisition software (Axon Instruments).

2.2.3 Data analyses

The extracellular signal was digitally low-pass filtered (Finite Impulse Response [FIR] filter) at 1 kHz and subjected to an additional high-pass FIR filtering at 100 Hz to distinguish CAPs. The selection of events was performed using filtered data superimposed on unfiltered data to ensure that filtering artifacts would not contaminate the analysis. Large amplitude (over ± 200 μV) oscillatory activity was considered CAP-like and was accepted into the analyses. The original 10 kHz data was additionally high-pass filtered at 200 Hz to identify stimulation artifacts. Since we used FIR filtering to prevent phase distortions, we could accurately combine the two differently filtered data to separate stimulation time-locked evoked CAPs from induced CAPs that were not temporally bound to stimulation. The first CAP occurred in a time window of 7-12 ms after a stimulation pulse and was considered evoked, whereas later CAPs of up to two seconds were counted as induced. Previous studies have indicated an approximate three-second timeframe between stimulation induced burst-like and epilepsy-like discharges (Gluckman et al. 2001). In addition, tetanically induced gamma oscillations do not extend beyond 1.5 s. Consequently, we discarded events occurring later than two seconds after the stimulation as epileptiform. In the intracellular recordings, only neurons with overshooting APs and resting membrane potentials below -55 mV were included in the analysis. The intracellular APs were classified accordingly.

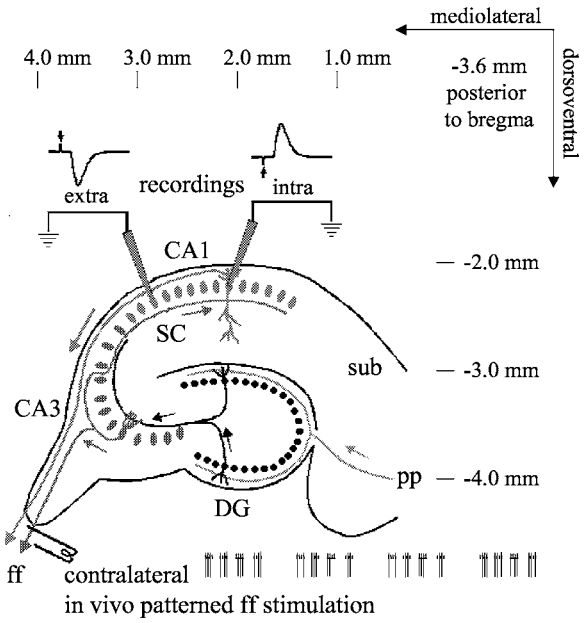

Figure 2.1 A schematic drawing of the hippocampus and its pathways demonstrating the extracellular and intracellular recording sites in CA1 area of the hippocampus and the contralateral fimbria-fornix stimulation projecting to the CA3 area. Briefly, the main input (from sensory modalities) to the hippocampus comes from the superficial layers of the entorhinal cortex (EC) along the perforant path (*pp*). *Pp* terminates in dentate gyrus (DG), which sends mossy fibers to cornu Ammonis layer 3 (CA3), which in turn projects to cornu Ammonis layer 1 (CA1) *via* the Schaffer collaterals (SC). The signal leaves the hippocampus *via* the subiculum (sub) and projects to the deep layers of the EC directly and *via* the subiculum. Note that *pp* has also direct projections to areas CA3 and CA1. Communication between the two hippocampi occurs partially *via* the fimbria-fornix (*ff*), which has afferents from CA3, CA1, and from more than 20 subcortical structures, including e.g. cholinergic and GABAergic afferents from the septum (Buzsaki et al. 1989). Arrows next to pathways indicate the direction of the current flow. Electrical *in vivo* gamma/theta -patterned stimulation (at the bottom) was used to stimulate *ff* contralateral to CA1 recordings. Note the slow 0.5 Hz cycles interrupting the stimulatory theta frequencies. Trains of vertical arrows here and in subsequent figures denote individual stimulation pulses at gamma and theta frequencies. Evoked responses occurred in CA1 at 7-12 ms latency from the *ff* stimulation. This indicates that the stimulation antidromically activated CA3, which subsequently activated CA1. Lowering one of the recording electrodes to CA3 verified this activation pathway (data not shown). The short traces above the recording electrodes indicate the polarity (positive up and negative down) of recorded action potentials in this and subsequent figures.

The instantaneous frequency was calculated from the interval between the negative (extracellular) or positive (intracellular) peaks of two consecutive induced CAPs or APs, respectively. The inter-spike interval data was then divided into gamma stimulation frequency groups. Data analysis consisted of computations of autocorrelations for each group and inter-group analysis using bivariate correlation analysis and one-way analysis of variance (1-way ANOVA) with a Tukey-test for pair-wise comparisons within the gamma band CAPs. We used SPSS 11 for Windows (SPSS Inc, Chicago, IL, USA) for the analyses.

2.3 Results

2.3.1 Extracellular gamma CAPs

In this experiment, extracellular and intracellular membrane potential changes and APs of the hippocampal CA1 cells were recorded in response to *in vivo* patterned fimbria-fornix stimulation epochs of embedded gamma, theta, and slow frequencies (Figs. 2.1-2.3). We shall refer to this stimulation paradigm as gamma/theta-patterned. Bragin et al. (1995) have shown that each theta cycle can contain approximately 10 gamma cycles. In order to create such a temporal structure, we embedded 4 gamma stimulation pulses into a theta cycle. In other words, we created an *in vivo* resembling situation where four stimulation gamma cycles and six "empty" gamma cycles constituted each theta cycle. The vertical arrows below recording traces in figures 2.2 and 2.3 demonstrate the groups of four stimulation gamma cycles and subsequent empty cycles. The stimulation part of the design corresponds to the depolarized phase of natural hippocampal theta oscillation when the firing of the neurons most likely occurs. Stimulatory theta frequency was similarly embedded into a slow 0.5 Hz frequency as depicted below the schematic illustration of hippocampus in figure 2.1. The slow frequency was implemented in order to reduce pulse numbers. In addition, the slow rhythm further emphasized the *in vivo* nature of the stimulations, since the hippocampal gamma oscillations have been shown to coincide with 0.5 Hz frequencies (Penttonen et al. 1999). In an epoch, each stimulation frequency band, gamma, theta, and slow, was repeated four times. Thus, a total of 64 stimulation pulses were applied at a given gamma frequency, but interspaced with non-stimulatory phases corresponding to theta and slow frequencies. In total, 1237 stimulation epochs from 371 10-minute sessions were recorded. Neither intensity nor frequency of the stimulation was varied during the course of the 64-pulse epoch. Although fimbria-fornix has connections to both CA1 and CA3 (Fig. 2.1), we did not observe direct stimulation effects in the CA1 area indicated as antidromic CAPs or APs 3-5 ms after the stimulation. However, antidromic CAPs (3-5 ms after the stimulation, and 4-7 ms before CA1 CAPs) were evident in the electrodes lowered into the CA3 area of the hippocampus (data not shown). The recordings were conducted in the gamma frequency order of low-high-low or high-low-high and randomly to reduce systematic error. The patterned stimulation-evoked CAPs in all sessions were recorded from 25 animals. Post-stimulatory, induced CAPs were evident in 85% (317) of the 10-minute recording sessions. In general, the patterned gamma/theta stimulation resulted in one or two induced CAPs retaining the periodicity of the stimulation gamma frequency. These CAPs appeared after the final stimulation pulse in a gamma series, delayed by the periodicity of the stimulation frequency. Additionally, in every animal, at least one recording exhibited a short burst of CAPs or prominent oscillations at or

close to (± 2.5 ms) the gamma stimulation interval (Fig. 2.3E and 2.2A; combining examples from six animals stimulated at 40 or 60 Hz gamma/theta -pattern). Experiments with higher than twice the threshold stimulations yielded similar results albeit with more frequently occurring double CAPs at 200 Hz and prolonged attenuation of the unit activity.

2.3.2 Intracellular gamma CAPs

Retention of the stimulation gamma periodicity was additionally present in 15 of the 20 intracellular recordings (Figs. 2.3 and 2.2B; four individual pyramidal cells stimulated with 40 Hz and 60 Hz gamma/theta -patterns). The five unresponsive cells may have been injured during the insertion of the electrode since, despite having overshooting APs, all of these cells were lost during the first 15 minutes of recording. Interestingly, the amplitude of the intracellular APs in the cells responding to the stimulation declined rapidly in the course of the gamma stimulations (Figs. 2.3A-C). The reduction in the AP amplitude coincided with the permanent depolarization (indicated by thick arrows in the Figs. 2.3B and C) of the cell membrane above the firing threshold of approximately -56 mV. The AP amplitudes recovered after the cell returned to normal membrane potential, or after it was hyperpolarized by current injection (data not shown). In general, the AP frequencies and burst durations were similar to the CAP responses described above.

Altering only the stimulatory theta frequency did not significantly affect induced CAP or AP frequencies. Rather, the induced gamma frequency was determined by the gamma component of the stimulation (Figs. 2.3D and E), and the induced theta frequency was 4.4 ± 1.6 Hz (s.e.m.) irrespective of the stimulatory theta or gamma frequencies. However, in experiments excluding the theta frequency, no retention of the gamma stimulation frequency was evident. Therefore, the underlying stimulatory theta frequency was necessary, at least for the detection of retention of the stimulatory gamma frequency, though it did not affect the frequency of that retention. Prolonged (10-20 s) stimulation epochs with an increased pulse number were tested in ten animals. In eight of these animals, the duration of CAP firing increased to tens of seconds, but the periodicity of the stimulation was no longer recognized. Even though there was a short-term retention of the stimulation periodicity evident in the CAPs during the initial phase of the prolonged stimulation, the prolonged responses declined to the beta frequency band (12-20 Hz) with interruptions at 1.4-2 Hz (fig. 2.3F). The findings on beta transition are in accordance with previous experiments (Pare et al. 1992; Pare and Llinas 1995). It has been suggested that this decline from gamma to beta frequencies may result from prolonged recovery from inhibition (Bracci et al. 1999; Traub et al. 1999a) or habituation (Whittington et al. 2000). By limiting the number of pulse sequences to four and additionally limiting the time frame of induced CAPs accepted into the analysis to two seconds, we eliminated the longer beta frequency afterdischarges from the analysis. In addition, tetanically induced gamma oscillations in CA1 *in vitro* have been shown to persist for up to 1.5 s, and are in the same range as the *in vivo* gamma oscillations induced by visual stimulation or those occurring spontaneously in monkey sensorimotor cortex (Traub et al. 1999a). Therefore, our CAP results display neuronal behavior that can be considered to fall within the limits of normal hippocampal physiology, although the phenomenon is mainly revealed at the population level.

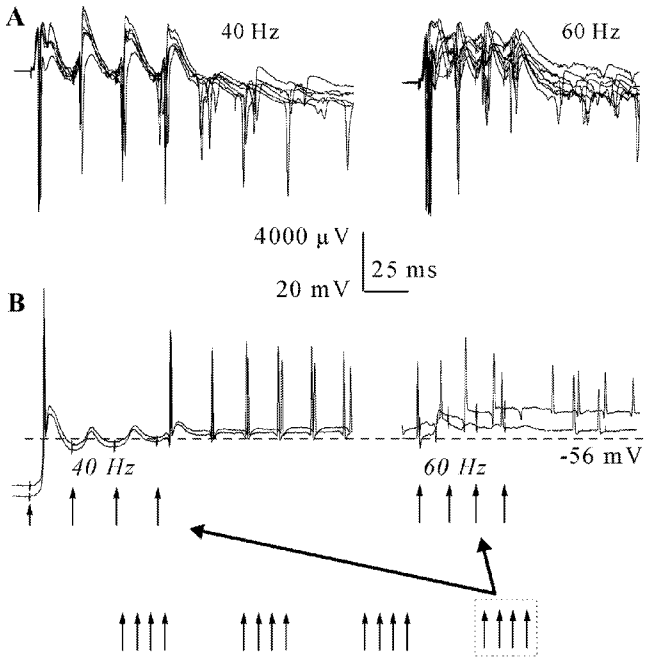

Figure 2.2 Cut traces from extracellular and intracellular recordings from hippocampal CA1 pyramidal cells in response to gamma/theta -patterned fimbria-fornix stimulation. Arrows below the figure illustrate the entire gamma/theta stimulation pattern, and indicate that only the last 4 pulses of stimulations are shown. Traces were not concurrently recorded. **A)** Superimposed wide-band (0.1 Hz- 6 kHz) recordings from 12 animals in response to 40 Hz (left) and 60 Hz (right) stimulation. Extracellular field potential recordings display retention of the periodicity of the stimulation in the compound action potential (CAP) timing. **B)** Superimposed intracellular recordings from four separate CA1 pyramidal cells stimulated with 40 Hz and 60 Hz gamma patterns demonstrating retention of stimulatory gamma frequencies in the post-stimulatory action potential (AP) timing. Note the variation in the amplitude and temporal relations both in the stimulatory and post-stimulatory CAP and AP responses. Note the prolonged silence (corresponding to 30 Hz subharmonic frequency) following the 60 Hz stimulations. The same animal (extracellular recordings) or cell (intracellular recordings) has been used only once at each frequency.

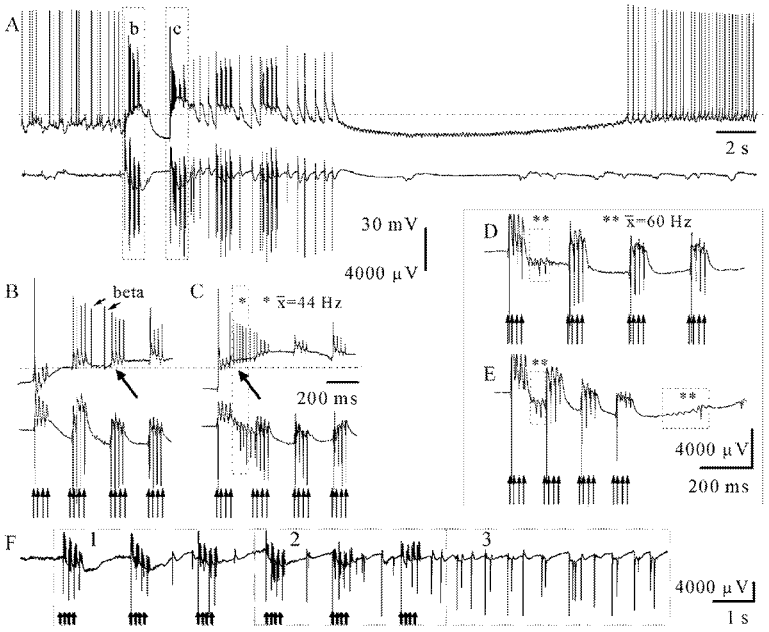

Figure 2.3 Extracellular and intracellular recordings from hippocampal CA1 pyramidal cells in response to gamma/theta -patterned fimbria-fornix stimulation. **A)** Concurrent intracellular and extracellular recordings from hippocampal area CA1 before, during, and after patterned gamma (40 Hz, 4 pulses), theta (4 Hz, 4 cycles), and slow (0.5 Hz, 4 cycles) stimulation. **B** and **C)** correspond to outlined areas (b and c) in **A** and illustrate, with a more extended time base, the different cycles of the stimulation. Note the stimulation uncorrelated beta frequency CAPs denoted by small arrows in (**B**) and the near stimulation frequency burst (indicated by *) inside the dashed box in (**C**). The dashed lines indicate the firing threshold (-56 mV), while arrows along the dashed lines indicate the points of sustained membrane depolarization above the firing threshold within each cycle. Note the coincidence of the permanent depolarization and the reduction in action potential (AP) amplitude (**B-C**). **D** and **E)** Extracellular recordings from a single animal during 60 Hz gamma stimulation patterned at 4 Hz (**D**) and 7.5 Hz (**E**) theta intervals. The last 16 pulses of the stimulations are shown. Note the induced CAPs and oscillations at 60 Hz (**) in dashed boxes corresponding to the stimulation gamma frequency. **F)** Extracellular recording during and after prolonged gamma/theta patterned stimulation comprised 6 gamma cycles (60 Hz), 4 theta cycles (6 Hz), and 6 slow cycles (0.5 Hz). The trace is divided into three sections (dashed boxes) demonstrating the stimulatory uncorrelated early phase (1), retention of the stimulation frequency (2), and the prolonged epileptiform afterdischarges at 10-20 Hz beta frequencies (3).

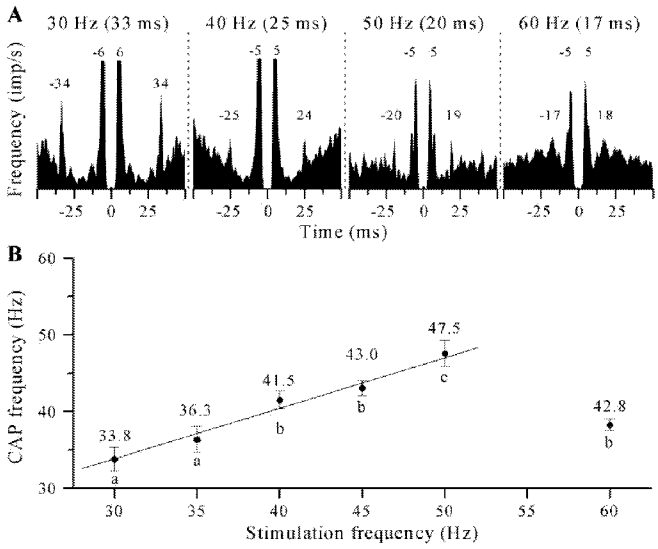

Figure 2.4 Mean compound action potential (CAP) responses to patterned gamma/theta stimulation from 25 animals. **A)** Autocorrelation function of CAP intervals after 30, 40, 50, and 60 Hz stimulation. All groups peak at 5 ms (corresponding to 200 Hz) and additionally at the stimulatory gamma frequency. Note the y-axis scale imp/s, the time from CAP peak to peak. **B)** Correlation analysis of mean gamma CAP frequencies. The correlation is significant in the middle and low gamma frequency range (Pearson correlation R2 = 0.96, $p < 0.01$). The dark dots represent the means with 95% confidence intervals. Above the dots are the exact values of the means (Hz). Any two stimulation frequency groups sharing a common letter (a, b or c) are not significantly different at $p < 0.05$ (1-way ANOVA, Tukey-test for pair-wise comparisons). Note the discrepancy in the 60 Hz stimulation group, where the autocorrelation function peaks at 60 Hz while the mean gamma CAP frequency is only 42.8 Hz, approaching the mean (45 Hz) of the 60 Hz stimulation frequency and its first subharmonic, 30 Hz.

2.3.3 Autocorrelation of stimulation frequency driven induced gamma frequency CAPs

To study the generality of the above results, the post-stimulatory induced CAPs of all the recorded animals were combined into gamma stimulation frequency groups for further analysis. In each group, the autocorrelation function of the data peaked at the stimulation frequency (Fig. 2.4A) and, as is typical of CA1 pyramidal neurons, at 200 Hz. We wanted to further specify the gamma response, and selected only the gamma frequency CAPs to study whether there were additional differences between the gamma stimulation frequency groups.

The results from 1-way ANOVA and correlation analysis (Fig. 2.4B) were similar to the results obtained from the autocorrelation functions. There was a tight correlation between

stimulatory and induced rhythms at gamma stimulation frequencies up to 50 Hz. The 60 Hz gamma stimulation frequency group, on the other hand, peaked in the autocorrelation function at 60 Hz, but showed a remarkably lower gamma frequency mean of 42.8 Hz. This can be explained by the inability of the anesthetized animal to repeat high frequencies (Penttonen, et al. 1998), and a subsequent increase in subharmonic firing since (60 Hz + 30 Hz) / 2 = 45 Hz. Indeed, the decline into subharmonic frequencies was more evident in the higher stimulatory gamma frequencies (data not shown). Furthermore, the artificial division of CAPs into a gamma frequency band from 20 to 70 Hz biased the results in favor of the lower frequencies.

2.4 Discussion

Previous experiments have described precise gamma synchronization in the hippocampal formation (Chrobak and Buzsaki 1998a; Fisahn et al. 1998; Penttonen et al. 1998; Bracci et al. 1999). Here, we have shown that not only are there synchronous gamma frequency ensembles in the hippocampus, but there is a capability to retain a gamma frequency pattern, defined by prior gamma/theta stimulation. This capability was demonstrated as the retention of the gamma periodicity of the *in vivo* patterned gamma/theta stimulation. The frequency of the underlying induced theta oscillation did not significantly interact with the gamma frequency retention. Furthermore, the induced CAPs were frequency locked into the gamma component of the stimulation, irrespective of the frequency of the underlying theta component of the stimulation. Therefore, the gamma/theta patterned fimbria-fornix stimulation did not affect the hippocampal theta frequency output in the structures primarily responsible for hippocampal theta activity, the entorhinal cortex (Ylinen et al. 1995b), medial septum (Dragoi et al. 1999) and raphe nucleus (Varga et al. 2002). In addition, CA3 has been identified as an intrahippocampal theta rhythm generator (Buzsaki 2002). In our recordings, CA3 may have influenced theta current generation, but it was unable to modify the frequency of the rhythm. On the other hand, our experiment was designed to reveal gamma frequency related changes in the hippocampus, and within each stimulation epoch we had 16 opportunities for induced retention of gamma frequencies compared to only 4 occasions for induced theta (Fig. 2.1). Interestingly, however, the theta component of the stimulation was necessary to induce gamma frequency firing.

Millisecond-range variability in the induced oscillation around the stimulatory gamma timing indicates that the mechanism of action is not precise within the sub-millisecond range. Such retention of temporal relations with an inbuilt degree of variability could be formed by depolarization level dependent resonance of the participating pyramidal neurons (Penttonen et al. 1998). The preservation of the temporal information may not be restricted to the pyramidal cell resonance in the CA1, but may incorporate other parts of the hippocampal formation that supply CA1 with excitatory or inhibitory inputs. The network drive imposed to the CA3 interconnections by the gamma/theta -patterned stimulation could be strong enough to locally override the synaptic suppression. Therefore, the induced stimulation frequency specific rhythm could be retained in the associative CA3 network and transmitted into CA1 after the stimulation. The proposed transfer of the rhythm from CA3 to CA1 has been described *in vitro* (Fisahn et al. 1998) and *in vivo* at a higher frequency band (Csicsvari et al. 2000).

The interneuronal network can operate at variable gamma frequencies depending on $GABA_A$ decay time and network properties at a given state (Whittington et al. 1995). Our gamma/theta -patterned stimulation could entrain the interneuronal network to oscillate at stimulatory gamma frequencies. If this oscillation persists beyond the end of the stimulation, the entrained set of interneurons could retain the frequency by rhythmic inhibition (Wang and Buzsaki 1996; McBain and Fisahn 2001). Since the intrinsic firing of the hippocampal interneurons occurs at gamma frequencies, this depolarization dependent interneuronal gamma frequency modulation would represent a cost-efficient way of achieving frequency retention in the hippocampus. The initial subharmonic CAPs evident in the right hand panels of figure 2.2 could result from increased interneuronal activity hyperpolarizing the pyramidal cells sufficiently to omit the first cycle of 60 Hz induced rhythm. In addition, the reduced level of glutamate-mediated excitation under urethane anesthesia (Heltovics et al. 1995) further emphasizes the role of the interneuronal network. The issue of interneuron actions *in vivo* should be further examined in future experiments.

The variation in the autocorrelation function suggests that not all the pyramidal cells in the CA1 area are driven into the rhythm, but the stimulation frequency is retained in groups of cells with possibly favorable intrinsic resonance or appropriate interneuronal connections (Wang and Buzsaki 1996). However, we could produce stimulation frequency specific population responses at varying gamma frequencies during a single recording. This indicates that the same pyramidal cells were receptive to different gamma frequencies. Furthermore, the intracellular recordings demonstrated that individual cells were responding accurately to several stimulatory gamma frequencies. Therefore, we are not selecting neurons responsive to specific frequencies, but rather tuning the peak frequency of the network. The hypothesis is further supported by the fact that CAPs retaining the periodicity of the stimulation frequency were sporadic. This is in accordance with previous experiments where pyramidal cells have been shown to fire in approximately 5 % of interneuronal gamma cycles (Whittington et al. 2000).

We have demonstrated a mechanism for short-term storage of the temporal structure of hippocampal oscillations. In our experiment, the CA1 hippocampal network retained the gamma periodicity of the *in vivo* patterned gamma/theta frequency stimulation. We believe this preservation of temporal relations evolves from the interplay between the underlying hippocampal interneuronal network and the associative reverberant connections between CA3 pyramidal cells. The intrinsic properties or resonance of the interneuronal network were able to repeat the periodicity of the gamma stimulation, whereas the pyramidal cells recovering from inhibition again excited the interneurons, thus reinforcing the induced rhythm. Since the fimbria-fornix stimulation had reduced the synaptic noise, this phenomenon was visible in the CA1 network. Given that the beginning of the stimulation temporarily suppresses the nerve cells (Figs. 2.3A and B), it is possible that this initial CAP firing is a result of the simultaneous recovery of the majority of the pyramidal cells. Therefore, the early uncorrelated spiking (spikes not entrained to the stimulation frequency, Fig. 2.3F, panel 1) could be due to the excitatory recurrent connections overriding the inhibition (Bragin et al.

1995). In contrast, later subharmonic action potentials most likely result from increased inhibitory interneuronal activation forcing the pyramidal cell membrane potential below the firing threshold during one or two consecutive gamma cycles (Wang and Buzsaki 1996). We conclude that the *in vivo* patterned gamma/theta stimulation induces short-term self-sustaining alterations in the temporal properties of the hippocampal CA3-CA1 network gamma oscillations. This dynamic retention of gamma timing could link the spatially synchronized cell assemblies into a single temporal domain in the hippocampus. Thus, the short-term temporal specificity would combine different units of the hippocampal neuronal network into a functional ensemble for effective information coding.

Chapter 3
Frequency bands and spatiotemporal dynamics of beta burst stimulation induced afterdischarges in rat hippocampus *in vivo*

Temporal and spatial characteristics of hippocampal neuronal network activation are modified during epileptiform afterdischarges. We developed a beta burst stimulation protocol to investigate subregional variations and substrates of rhythmic population spike discharges *in vivo* in urethane anesthetized Wistar rat hippocampus with a 14-electrode recording array and extracellular single electrode recordings. Our 64 pulse beta burst stimulation protocol was constructed from electrical pulses delivered at intervals corresponding to beta (14-25 Hz), delta (2 Hz), and slow (0.5 Hz) frequencies. In each experiment these interleaved pulses were all repeated four times with intervals unchanged. Stimulation of either perforant path or fimbria-fornix induced a prolonged afterdischarge pattern peaking at 200 Hz fast, 20 Hz beta, and 2 Hz delta frequencies. Analysis of variance confirmed that response pattern of the discharges remained constant regardless of the stimulation beta frequency. Within the afterdischarge the fast frequencies were restricted to independent hippocampal subfields whereas beta and slow frequencies correlated across the subfields. Current source density (CSD) analysis revealed that the original signal propagation through subfields of the hippocampus was compromised during the beta burst stimulation induced afterdischarge. In addition, the CSD profile of the epileptiform afterdischarge was consistently similar across the different experiments. Time-frequency analysis revealed that the beta frequency afterdischarge was initiated and terminated at higher gamma (30-80 Hz) frequencies. However, the alterations in the CSD profile of the hippocampus coincided with the beta frequency dominated discharges. We propose that hippocampal epileptiform activity at fast, beta and delta frequencies represents coupled oscillators at respectively increasing spatial scales in the hippocampal neuronal network *in vivo*.

3.1 Introduction

Investigation of the transition between normal and abnormal brain states provides insight into the network architecture and function of the brain. One way to understand neuronal networks is to examine disturbances in the electrical network of the brain during epilepsy or epileptiform brain states. Thus, periodic ultra-synchronous discharges of large neuronal ensembles are the hallmark of various epileptic conditions (McCormick and Contreras 2001), and the study of the initial conditions of such discharges can provide information on normal brain function, as well as elucidate the mechanisms involved in the generation of epileptiform activity. Hippocampus is an important focus of epileptic activity in humans and in some animal models of temporal lobe epilepsy (McCormick and Contreras 2001; Jefferys 2003). Therefore, it seemed appropriate to study the mechanisms of the emergence of afterdischarges in the hippocampal neuronal networks. Epilepsy related functional reorganization of the hippocampal network can be examined *via* the electrical properties of the network. To date, the *in vivo* methodology of local field potential recording offers the most complete tool to investigate normal or pathological fast network interactions in the intact brain.

Within normal brain states, the beta and delta frequencies have been associated with epilepsy prone internal brain activity, such as 14 Hz sleep spindles in the thalamus (Steriade et al. 1993), synchronized activity in prefrontal cortex (Liang et al. 2002), and hippocampal memory consolidation during slow wave sleep (Buzsaki 1989; Sirota et al. 2003). Cavazos et al. (1994), Amzica and Steriade (1999), and Hirai et al. (1999) have also reported beta frequencies occurring in epileptic conditions *in vivo*. It has been claimed that beta frequency stimulation can either induce epileptiform activity (Somjen et al. 1985; Lothman and Williamson 1992) or that after the epileptiform synchrony has developed, one of its hallmarks is beta frequency bursting (Pare et al. 1992; Bragin et al. 1997; Amzica and Steriade 1999; (Hirai et al. 1999; Medvedev et al. 2000). However, only a few experiments have been conducted linking the beta frequency induction of paroxysmal afterdischarges into the epileptiform beta frequency outcome of the stimulation (Amzica and Steriade 1999). Furthermore, Bikson et al. (2003) have demonstrated that paroxysmal beta frequencies are at least initially accompanied with fast, >80 Hz, oscillations whereas Pare et al. (1992) and Steriade and Contreras (1998) have reported delta frequencies co-occurring with beta frequencies in already epileptiform conditions.

A systematic investigation of an epileptiform afterdischarge with time-sensitive interactions involving more than two frequency bands would provide novel information about the temporal structure and frequency division of the afterdischarge and facilitate the understanding of the mechanisms behind the development of the epileptiform afterdischarge. Here we report brief beta burst stimulation induced epileptiform afterdischarges in rat hippocampus *in vivo* co-occurring at anatomically distinct scales and at three frequency bands.

3.2 Methods

3.2.1 Animals

Experiments were conducted on 20 male Kuopio Wistar rats (250-350 g) anesthetized with 1.1-1.4 g/kg urethane. The methods used in the experiments were approved by the State Provincial Office of Eastern Finland (approval number 99-61).

3.2.2 Surgical procedures

Animals were placed in a stereotaxic instrument, the scalp was removed, and small bone windows were drilled above the target structures. Two separate paradigms were used in the recordings, illustrated as A and B in figure 3.1. Paradigm A consisted of single electrode (60 μm tungsten wire) recordings of local field potentials from the pyramidal cell layer of the CA1 field of the hippocampus (-3.6 mm anteroposterior and -2.2 mm lateral to bregma, 15 animals). Paradigm B consisted of 14 channel (16-channel silicon probe with 100 μm recording site separation, courtesy of University of Michigan Center for Neural Communication Technology, MI, USA) recordings perpendicular to the hippocampal subfields (-3.6 mm anteroposterior and -4.0 mm lateral to bregma with a 30° angle towards midline, 5 animals) to monitor principal cell layers of dentate gyrus (DG) and CA1 as well as CA1 apical dendrites. Due to the limitations of a vertical recording array we were restrained

to record DG and CA1 omitting the CA3 region connecting the recorded areas. In both paradigms, a pair of stainless steel wires (100 μm in diameter) with 0.2-0.4 mm tip separation was placed in the fimbria-fornix (-1.3 mm anteroposterior and +1.0 mm lateral to bregma, and -4.0 mm ventral from cortical brain surface) to stimulate antidromically the commissural efferents of the contralateral CA3 region. In paradigm B, an additional pair of steel wires was placed -7.0 mm anteroposterior and -4.0 mm lateral to bregma and -3.0 mm ventral from cortical brain surface to stimulate the perforant path.

3.2.3 Stimulations and recordings

We used 0.2 ms electrical pulse stimulation (Master8 pulse generator and Iso-flex stimulus isolator, A.M.P.I, Jerusalem, Israel) at an intensity that was twice the threshold capable of inducing population spikes in more than two consecutive trials for both stimulation sites. The stimulation intensity was 300-600 μA. Vertical positioning to the CA1 pyramidal layer for the single channel extracellular and 14-channel silicon probe recordings was estimated from the polarity of the field response, the shape and firing patterns of the population spikes (Markram et al. 1997), and from the latency of the evoked field response and population spikes. Typically the CA1 pyramidal layer was located -2.0 ± 0.1 mm below the cortical surface. Additionally, we used CSD analysis to confirm the positions of the hippocampal subfields in the silicon probe experiments. Two stainless steel watch screws, driven into the bone above the cerebellum served as indifferent and ground electrodes in the recordings.

We used a modified stimulation paradigm from (Mikkonen et al. 2002) with different frequency ranges. Briefly, the stimulation consisted of four 0.2 ms pulses delivered at frequencies from 14-25 Hz with two underlying frequencies at 2 Hz and 0.5 Hz. Thus, we constructed a hierarchical stimulation that consisted of three interwoven frequency bands, slow, delta, and beta, each repeating 4 times and yielding a total stimulation of 64 pulses (Fig. 3.1). In order to maintain the stimulation intensity at a comparable level across the stimulations the beta stimulation frequency was designed to cover merely central part of the frequency band (14-25 Hz out of 10-30 Hz). The stimulation was repeated every 10 min. Every two hours there was an additional 30 min recovery period with no stimulation. If afterdischarges had not developed after two hours of stimulations, the number of stimulation pulses at each beta sequence was increased to six. The stimulation paradigm was designed using frequency ranges co-occurring in slow wave sleep (Buzsaki 1989) and epilepsy (Timofeev et al. 1998; Amzica and Steriade 1999). Furthermore, grouping stimulation pulses interleaved with silent episodes provided a timeframe for the examination of the early development of paroxysmal afterdischarges (Mikkonen et al. 2002).

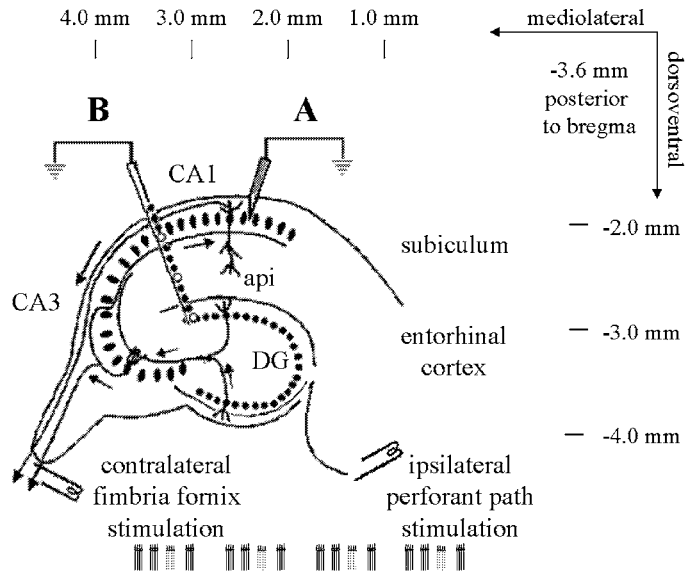

Fig. 3.1 Structure of the hippocampus including an illustration of the recording and stimulation sites within the hippocampus. Recordings were performed with a single electrode from CA1 2.2 mm mediolaterally from the midline **(setup A)** or with a 16 channel silicon probe in a 30° angle 4 mm mediolaterally from the midline **(setup B)**. CA1 pyramidal cell layer (CA1), CA1 apical dendrites (api), and the granule cell layer of dentate gyrus (DG) are shown in the hippocampus. Stimulation electrodes were inserted into contralateral fimbria-fornix (**A** and **B**) and into ipsilateral perforant path (**B**) for *in vivo* -periodic electrical beta burst stimulation at twice the threshold necessary to evoke a population spike. The temporal structure of the stimulation (14-20 Hz, 2 Hz, and 0.5 Hz) is schematically illustrated at the bottom of the figure.

The multichannel extracellular signals were first 500-fold amplified using Multichannel Systems (Reutlingen, Germany) amplifiers (two MPA-8s and one PA-32-D). The signals were then filtered between 0.1 and 5000 Hz (PA-32-D). Single electrode recordings were filtered between 0.1 and 6000 Hz using Cyberamp380 (Axon Instruments, Union City, CA, USA). Finally, all the signals were sampled with 16-bit precision (Digidata 1320A; Axon Instruments) at 10 kHz (single channel recordings) or 12.5 kHz (multichannel recordings). The data were stored on a computer hard disk using Axoscope 8.0 data acquisition software (Axon Instruments). The data analyses were performed offline using Clampfit 9.0 (Axon Instruments), Matlab 6.5 (MathWorks Inc, Natick, MA, USA), and SPSS 11 for Windows (SPSS Inc, Chicago, IL, USA).

The single channel extracellular signal recorded from CA1 pyramidal layer was used to compare instantaneous firing frequencies within afterdischarges against stimulation frequencies (Mikkonen et al. 2002). The signal was digitally low-pass filtered (finite impulse response filter) at 500 Hz, downsampled to 1 kHz, and subjected to an additional high-pass finite impulse response filtering at 100 Hz to distinguish population spikes.

3.2.4 Data analyses

The instantaneous frequency was calculated from the interval between the negative peaks of two consecutive population spikes. The selection of events was performed using filtered data superimposed on unfiltered data to ensure that possible filtering artifacts would not contaminate the analysis. The population spike interval data from 15 animals was then pooled and subsequently grouped according to stimulation beta burst frequency. We conducted a one-way analysis of variance (SPSS Inc) against the stimulation frequencies to define stimulation frequency dependent differences in mean frequencies across frequency bands. Tukey -test was used for Post Hoc analyses.

CSD analysis was calculated according to (Freeman and Nicholson 1975) in Matlab (MathWorks Inc). The CSD was calculated as

$$CSD(z) = [\ (2f(z) - f(z+\Delta z) - f(z-\Delta z)\ ]\ \sigma z\ /\ (\Delta z)^2, \quad (1)$$

where $CSD(z)$ is the CSD at depth z, $f(z)$ is the local field potential at depth z, Δz is the depth interval (Timofeev and Steriade 1997) and σz is the conductivity along the shaft of the 16-channel recording electrode. Conductivity was not measured during the experiments, but was considered as constant across hippocampal subfields. The resulting error can be considered as negligible with respect to the kind of results we sought (Holsheimer 1987; Wadman et al. 1992; Kaibara and Leung 1993). Thus, CSDs were calculated in arbitrary units (mV/mm^2), proportional to the actual current densities (Kaibara and Leung 1993). Averaged 50 ms CSDs were calculated from four 20 second epileptiform afterdischarges and traces of non-epileptiform evoked potentials of equal length.

Autocorrelation and coherence were calculated for tenfold downsampled signals using Matlab signal processing toolbox (MathWorks Inc). Autocorrelation was calculated on CA1 inter-spike interval data pooled from 8 animals. Only events occurring later than two seconds after cessation of the stimulation were considered as discharges and included into the autocorrelation analysis. The statistical significance of the correlation was evaluated between frequency bands using one-way analysis of variance (SPSS Inc). For coherence, signals corresponding to CA1 and DG were pre-selected on the basis of the CSD analysis. Coherence was calculated on 20 s mean epileptiform voltage trace pooled from three perforant path and fimbria-fornix stimulations. The window for the analysis was 1 s and it was moved a sample at a time across the entire 20 s signal. Three 20 s voltage traces of spontaneous oscillations collected prior to the stimulation experiments were used as reference for normal coherence under urethane anesthesia. Standard error of mean described the inter-discharge variation.

For time-frequency analysis we used wavelets on CA1 voltage data downsampled to 1 kHz. Time-frequency analysis was calculated in Matlab (MathWorks Inc) according to (Muthuswamy and Thakor 1998). Morlet wavelets were calculated from 0.1 Hz to 60 Hz with 0.1 Hz resolution in frequency domain and 1 kHz resolution in temporal domain. We imaged both spontaneous oscillations an individual afterdischarge to demonstrate the differences in the intensity and frequency distribution between normal and epileptiform *in vivo* rhythms of urethane anesthetized rat hippocampus.

3.3 Results

Stimulation paradigm of the experiment (Fig. 3.1) was designed to correspond to the frequency relationships between different epileptic oscillatory brain states (Pare et al. 1992; Steriade and Contreras 1998; Bikson et al. 2003). Beta burst stimulation delivered at ten minute intervals at twice the threshold capable of inducing population spikes was sufficient to drive the hippocampal neuronal network into epileptiform state during the first two hours of the stimulations in all but one of the recorded animals. We defined the emergence of a depolarizing shift as the beginning of an afterdischarge (Somjen et al. 1985). The afterdischarges always initiated first at DG regardless of the stimulation site. In addition, the population excitatory postsynaptic potentials increased three-fold at the initiation of the afterdischarge (data not shown). On each recording day, both fimbria-fornix and perforant path stimulations were continued until induced afterdischarges emerged. Inter-animal variance between trials was too large to reveal any differences in the afterdischarge thresholds between different stimulation sites. In general, three to six 64 pulse stimulation series with ten minute intervals were required before the afterdischarges emerged.

3.3.1 CSD analysis

CSDs were used to identify different hippocampal subfields. In addition, CSD analysis was used to evaluate the propagation of field potentials and discharges during and after the stimulations (Fig. 3.2) and averaged to accurately describe the locations of sources and sinks (Fig. 3.3). Thereafter, discharges were classified according to the CSD analysis. The first DG population spikes induced by perforant path stimulation did not propagate from DG to CA1 (Figs. 3.2A and 3.3A). However, perforant path stimulation induced a minute population spike in CA1 5 ms after the stimulation. Fimbria-fornix stimulation, on the other hand, induced immediate population spikes at CA1 (Fig. 3.3C), but did not induce DG firing until 5-8 seconds later (Fig. 3.2D). At the emergence of the epileptiform afterdischarge the propagation profile transformed as described in Somjen et al. (1985). The early discharges still had the overall temporal profile of the normal transmission of action potentials through the hippocampal trisynaptic loop. Five seconds from the onset of the afterdischarge the temporal sequence of events was already compromised as evidenced by the nearly vertical dashed lines indicating the individual population spikes in Figs. 3.2B and E.

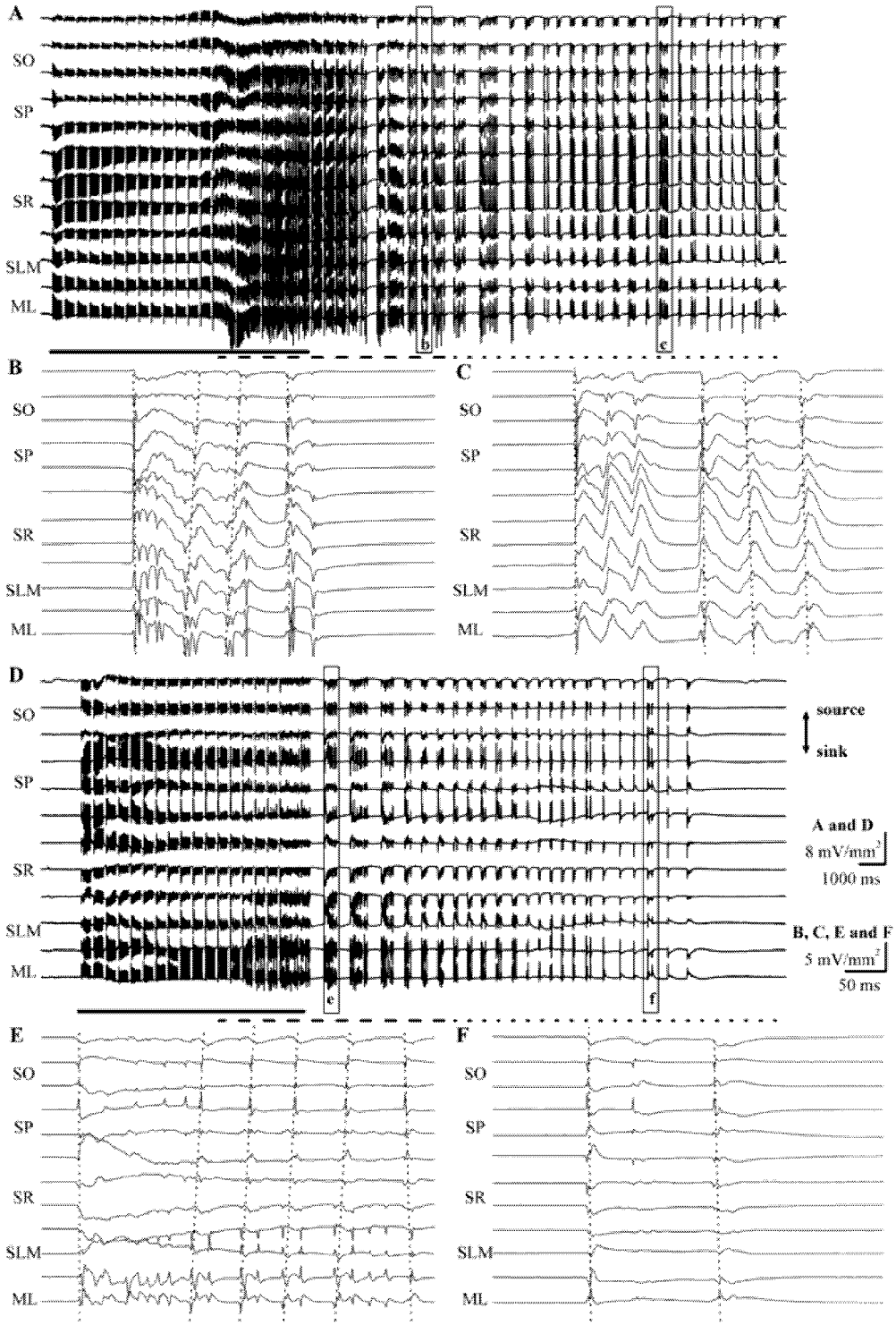
A
SO
SP
SR
SLM
ML
b
c
B
C
D
e
f
source
sink
A and D
8 mV/mm²
1000 ms
B, C, E and F
5 mV/mm²
50 ms
E
F

Fig. 3.2 CSD analysis of beta burst stimulation induced afterdischarge switching from synaptic propagation into region specific, nearly synchronous discharges in hippocampus. **A** and **D)** CSD clips of 12 channels from epileptiform afterdischarge induced by 20 Hz beta burst stimulation of perforant path (**A**) and fimbria-fornix (**D**). Here, and in subsequent figures, the time of the stimulation is indicated as a solid black line, the temporal span of discharges that propagate in temporally normal order is presented as a dashed line and the nearly simultaneous regionally independent discharges between the hippocampal subfields are indicated as a dotted line. Note the depolarizing wave at 6 s (**A**) and 2 s (**D**) initiating the afterdischarges. The symbols on the left of the trace in this and subsequent figures denote *stratum oriens* (SO), *s. pyramidale* (SP), *s. radiatum* (SR), *s. lacunosum moleculare* (SLM), and molecular layer of the DG (ML). Note the different initial response patterns governed by SLM and ML in perforant path stimulation (**A**) and SP and SR in fimbria-fornix stimulation (**D**). Note also that although the discharge patterns and temporal relations of the different stimulations are similar, the SLM is source in perforant path stimulation (**A**) and sink in fimbria-fornix stimulation (**D**). Note also the differential slow wave changes in the current-depth profiles between stimulation sites. Dashed boxes around the trace indicate the time points of the magnified insets **B**, **C**, **E** and **F**. **B** and **E)** The initial discharge initiates at DG and the CA1 population spikes are mainly synaptically mediated indicated by dashed lines originating at DG and propagating into CA1. Note that the first population spike discharge of each burst is simultaneous at DG and CA1. The subsequent discharges in the burst have irregular time difference between DG and CA1. **C** and **F)** The delayed discharge is composed of region specific and nearly synchronous discharges at CA1 and DG. In addition, an increase in size and duration of the apical dendritic sinks in SR is associated with the epileptiform discharges. Note the minute variation in the time-lags between the different hippocampal subfields and the changes in the direction of the discharge propagation, where CA1 population spikes can precede DG, or *vice versa*.

As reported previously (see (Jefferys 2003) for review), the temporal differences between hippocampal subfields vanished during the progression of the self-sustained epileptiform afterdischarge and were completely replaced by region specific and nearly synchronous population spike sinks in the hippocampal subfields irrespective of the stimulation site (Figs. 3.2C, 3.2F, 3.3B, and 3.3D). The CA1 basal dendritic sinks increased as the time difference between DG and CA1 spike discharges decreased (compare Fig. 3.2B to 3.2C and 3.2E to 3.2F). These large basal sinks can also be seen in averaged CSDs after fimbria-fornix stimulation (Fig. 3.3C) and during epileptiform afterdischarges (Figs. 3.3B and D). Additionally, the origin of the synchronous population spike discharge sinks varied between DG and CA1 (Figs. 3.2B, C, E, and F). Interestingly, the average profiles of perforant path and fimbria-fornix stimulation induced afterdischarges were identical and resembled the CSD profile of the non-epileptiform evoked fimbria-fornix stimulation (Fig. 3.3). Since the overall profiles and frequencies of the epileptiform afterdischarges obtained by stimulating perforant path and fimbria-fornix were inherently similar, they have been pooled in the subsequent analyses.

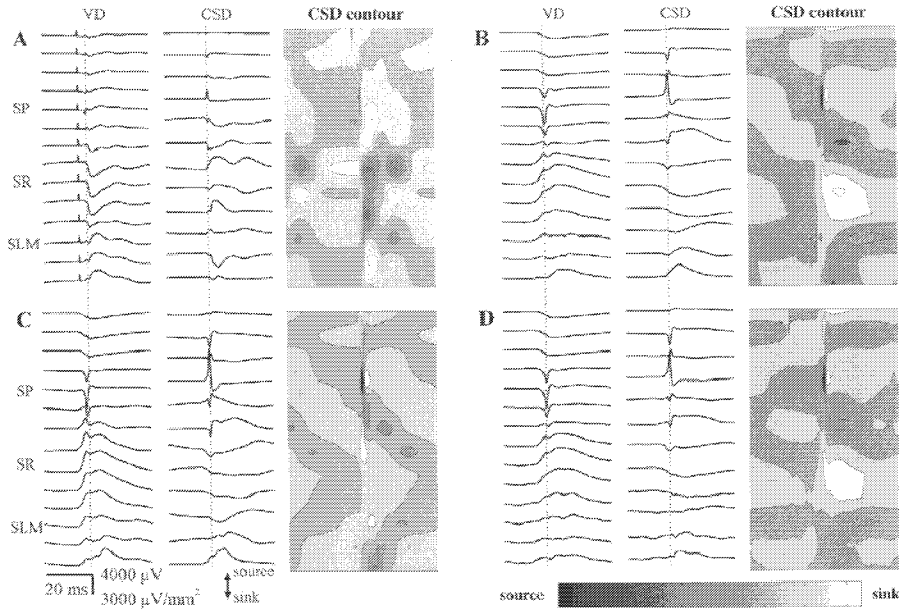

Fig. 3.3 CSD analysis of the averaged evoked and epileptiform spikes. Each trace is an average of 200 50 ms sweeps from 2 separate measurements. Notations on top of the figure denote voltage trace (VD) and current source density (CSD). Vertical dotted line in each subfigure indicates the position of the CA1 population spike peak used to trigger the averages. **A)** Evoked response to perforant path stimulation. Perforant path stimulation induced a sink in SLM and sources in SR, but there was no population spike in CA1. Note the small population spike in CA1 5 ms after the stimulation, which may indicate a direct entorhinal connection. **B)** Epileptiform response to perforant path stimulation. Epileptiform afterdischarge had a population spike in SP and the large sink in SR. **C)** Evoked response to fimbria-fornix stimulation. Fimbria-fornix stimulation evoked a population spike related sink in SP and a small sink in proximal SR. Note also that the stimulation artifacts have nearly vanished due to the averaging. **D)** Epileptiform response to fimbria-fornix stimulation. Epileptiform afterdischarge had a population spike associated sink in SP and the large sink in SR. Note also the minute sink in SLM. Note also the remarkable similarity between **B** and **D** as well as their close resemblance to **C**.

3.3.2 Stimulation frequencies

One-way analysis of variance was calculated for epileptiform spike discharge intervals from CA1 voltage recordings from 20 animals. Population spike intervals were defined as the time difference between two consecutive population spikes (N=3071) for the whole time series of all beta burst stimulation frequencies after removal of stimulation artifacts. The variance analysis revealed no significant differences in population spike discharge frequencies between different stimulation frequencies. We wanted to further examine the frequency profile of the discharges by grouping them into five frequency groups: delta, theta, beta, gamma, and fast. Beta frequency discharges accounted for 46% of all the frequencies assigning beta frequencies as the single largest group of the analysis at every stimulation frequency. For beta

frequency band, mean (±95% confidence intervals) afterdischarge frequencies were 20.9±2.3 Hz, 19.7±3.3 Hz, and 20.7±1.9 Hz, respectively for 14, 17, and 20 Hz stimulation frequencies. A change of the stimulation beta frequency between 14, 17, and 20 Hz had no effect on the prevalence of the afterdischarges.

3.3.3 Discharge frequencies

Autocorrelation analyses were conducted for extracellular single channel recordings of beta burst stimulation induced CA1 afterdischarges pooled from 8 animals with the longest afterdischarges (Fig. 3.4). For autocorrelation analysis, only discharges occurring two seconds after the cessation of the stimulation were included into the analysis. Therefore, the autocorrelation data was not contaminated by any stimulatory artifacts.

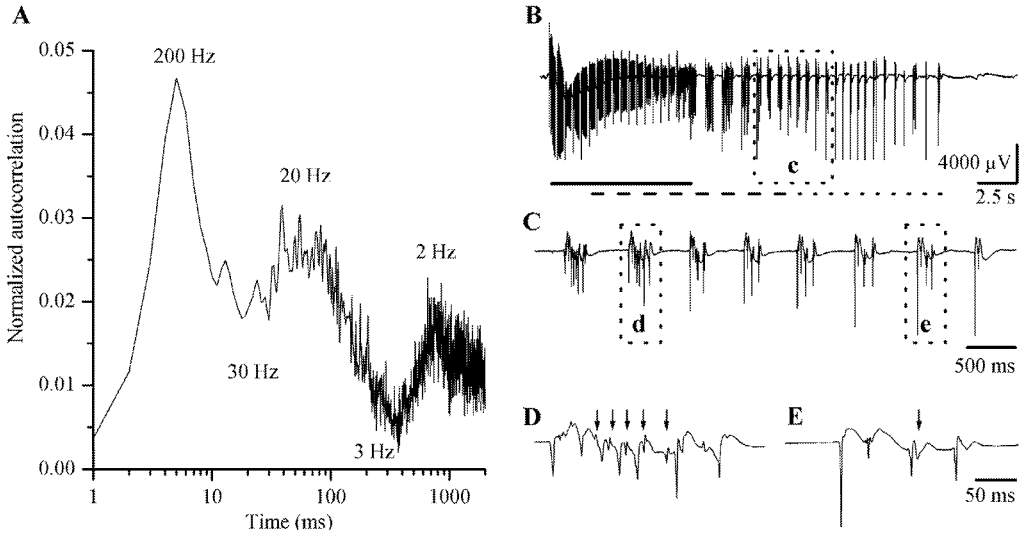

Fig. 3.4 Autocorrelation of CA1 population spike discharges after beta burst stimulation pooled from eight animals. **A)** Autocorrelation of the discharges. Note the logarithmic scale on x-axis. First two seconds of the afterdischarges were omitted from the analysis in order to obtain discharges that did not contain stimulatory artifacts or desynchrony from transition into epileptiform state. Note the peaks at 200, 20, and 2 Hz positions and dampening of the signal at gamma and theta frequencies. The numbered frequency bands have autocorrelations that are significantly different (one-way analysis of variance, $N = 831$, $p < 0.05$). **B)** An example of the afterdischarge. See Fig. 3.2 for details of the lines beneath the figure. Dashed box around the trace indicates the time point of the magnified inset **C**. **C)** Inset from B indicating the 2 Hz slow frequency. Dashed boxes around the trace indicate the time points of the magnified insets **D** and **E**. **D)** Inset from **C** indicating the fast 200 Hz activity in the CA1 as vertical arrows. Note also the gamma frequency spikes present in the beginning of the afterdischarge and their transitioning into beta frequencies. **E)** Inset from **C** demonstrating the beta frequency discharges.

Autocorrelation demonstrated that beta burst stimulation induced epileptiform afterdischarges peaking at 200, 20, and 2 Hz (Fig. 3.4A). The profile of the afterdischarge is presented in Fig.

3.4B, whereas the 2 Hz delta frequencies can be seen in Fig. 3.4C. Fig. 3.4D demonstrates the 200 Hz frequencies and the early gamma frequency bursting. The second spike in the 200 Hz fast frequencies was usually smaller than the first spike. The steady beta frequency component within the afterdischarge is exemplified in Fig. 3.4E. Interestingly, although gamma frequency firing was present in the beginning of the afterdischarge (Fig. 3.4D), the autocorrelation demonstrated a relative reduction of incidences at gamma and theta frequencies.

3.3.4 Coherence during the epileptiform afterdischarge

In order to study the development of the ultra-synchronous events across the hippocampal subfields, tenfold downsampled epileptiform voltage traces pre-selected on the basis of CSD analysis and corresponding to the principal cell layers of CA1 and DG were selected for coherence analysis (Fig. 3.5). Fig. 3.5A, pooled from three animals, demonstrates that in spontaneous oscillations in rat hippocampus under urethane anesthesia gamma frequencies are prevalent and the coherence values are lower compared to afterdischarges. Figure 3.5B demonstrates the pooled coherence from three epileptiform afterdischarges. The coherence is strong at slow and beta frequencies, but there is little coherence at gamma or high frequencies. Note also the slight drop in the coherence at theta frequencies in Fig. 3.5B.

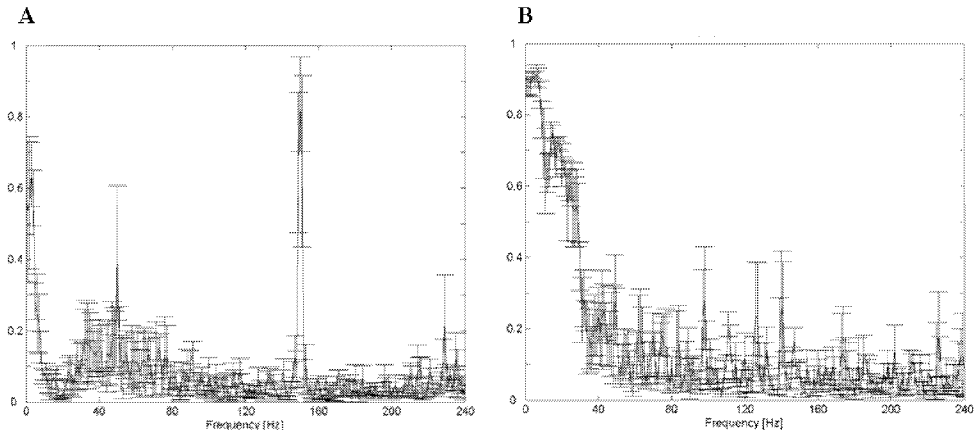

Fig. 3.5 Coherence analysis of normal and epileptiform rat hippocampus. **A)** Coherence of three 20 s traces of spontaneous field potentials from CA1 and DG. During spontaneous oscillations under urethane anesthesia coherence values peak at slow and gamma frequencies. Note also the 50 and 150 Hz interference from fluorescent lamps. **B)** Coherence (± s.e.m.) of three afterdischarges recorded from CA1 and DG. During the afterdischarges the coherence at delta and beta frequencies is high, but declines rapidly at gamma frequencies. Note also the slight reduction of coherence at theta frequency.

3.3.5 Temporal succession of alterations in the frequency content of the afterdischarge

We wanted to monitor the epileptiform afterdischarge simultaneously in frequency and time in order to capture the temporal structure of the alterations in frequency domain. The time-frequency analysis was calculated using wavelets (Muthuswamy and Thakor 1998). To visualize the differences between normal and epileptiform CA1 activity we imaged a spontaneous 20 s trace of local field potentials (Figs. 3.6 A and B) and a single epileptiform afterdischarge (Figs. 3.6 C and D). These results are applicable to all 20 animals recorded. The field potentials mainly consisted of theta frequencies (Fig. 3.6 B). In the afterdischarge, there was an initial discharge at gamma frequencies coinciding with the depolarizing shift (Figs. 3.6 C and D, starting from line i). Next the gamma discharge was accompanied by an increasing beta frequency component and a delta frequency pattern emerged (Figs. 3.6 C and D, line d). Thereafter the discharge transitioned into a prolonged and steady beta frequency discharge (Figs. 3.6 C and D, line b). Finally the afterdischarge terminated at a weaker burst of gamma frequencies.

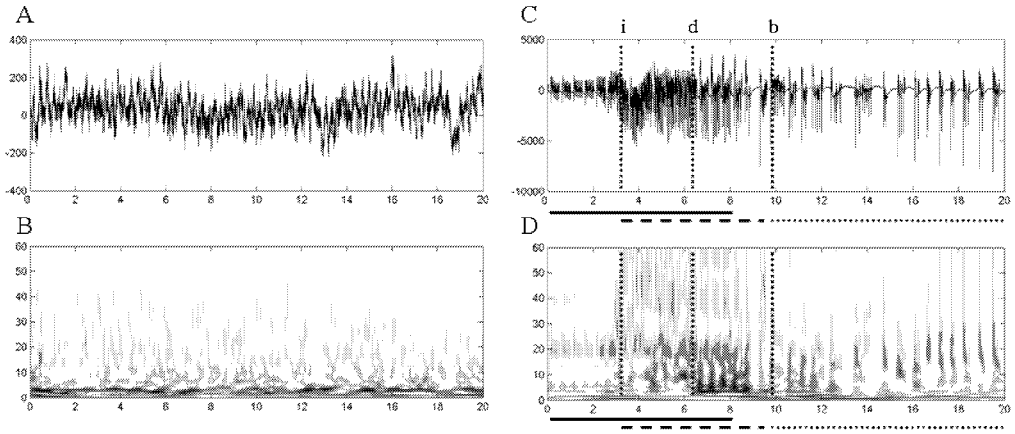

Fig. 3.6 Time-frequency evolution of the CA1 voltage traces by wavelet transformation. **A)** A voltage trace of spontaneous oscillations recorded from CA1. **B)** A wavelet transformation of **A**. Note the strong theta frequency oscillation. **C)** A voltage trace of CA1 epileptiform discharges. **D)** A wavelet transformation of **C**. The vertical dotted lines in **C** and **D** indicate the timing of the frequency switches associated with initiation of the discharge (i), emergence of delta rhythm (d), and the steady beta frequency discharge (b). See Fig. 3.2 for details of the lines beneath **C** and **D**. The discharges are characterized by strong delta and beta frequency drives. In addition, initial and terminal phases of the discharges are accompanied by gamma frequencies that are higher harmonics of the underlining beta frequency drive.

3.4 Discussion

Analysis of discharges of ensembles of neurons firing in unison provides a time-sensitive means to investigate the emergence of synchronized neuronal activity. We aimed to benefit from the temporal accuracy of these discharges within hippocampal subfields to examine the emergence of epileptiform afterdischarges at different frequency bands. Our results show that beta burst stimulation efficiently induces epileptiform afterdischarges in urethane

anesthetized rat hippocampus *in vivo*. These afterdischarges consist of early and late phases of gamma frequency discharges that border a prolonged discharge at 200 Hz fast, 20 Hz beta and 2 Hz delta frequencies. These states seem to be mutually exclusive.

Although we artificially induced epileptiform afterdischarges using stimulation bursts at beta and delta frequencies, the initial innate neuronal network response of the hippocampus was a discharge at gamma frequencies. Therefore, the necessary conditions for the epileptiform afterdischarge were generated by the beta burst stimulation, but the innate neuronal network generated gamma frequency discharges were required for the emergence of the actual epileptiform afterdischarge at fast, beta, and delta frequencies.

Our patterned beta burst stimulation resembles previous fast kindling protocols (e.g. (Bragin et al. 1997a), but benefits from the natural brain oscillations in the temporal structure of the stimulation and, furthermore, restricts the number of stimulation pulses into 384 in an hour and 2304 in a typical six hour recording day. In this study we focused on maintaining the overall intensity of the stimulation as constant as possible and varied the stimulatory beta frequency only at the central frequencies of the beta frequency band. At our selection of frequencies the alteration of the stimulation frequency in the beta burst had no observable effect on the prevalence or frequency of the consecutive afterdischarges. Our beta burst model was able to induce epileptiform afterdischarges lasting over ten seconds with three series of 64 stimulation pulses in naïve rats under urethane anesthesia even though urethane is known to suppress glutamatergic transmission and promote anticonvulsive effects (Heltovics et al. 1995). Lothman and Williamson (1992) demonstrated that similar numbers of stimulations delivered without patterning could induce afterdischarges in already kindled rat. The fact that the 64 pulse stimulation series was to be repeated three times with ten minute intervals before afterdischarges emerged suggests that some slow changes take place within the brain to allow excessive excitation and epileptiform discharges. In other words, the overall duration of the stimulation must reach a critical threshold before afterdischarge can develop (Lothman and Williamson 1992). Nevertheless, our beta burst model shows that the efficacy of the stimulation can be improved by proper patterning of the stimulation pulses.

Both perforant path and fimbria-fornix stimulations induced similar afterdischarges in the hippocampal neuronal network. During the stimulation of both sites the afterdischarge had a large sink in distal *stratum radiatum* (SR) evidenced by the CSD analysis. Similarly, the voltage traces demonstrated that CA1 was more profoundly activated than DG. The overall CSD profile of the afterdischarges resembled the profile from evoked non-epileptic fimbria-fornix stimulation. However, the sinks in SR were stronger and longer and more distal during the epileptiform afterdischarges. The increased duration of the SR sink indicate reduced $GABA_A$ mediated inhibition in CA3-CA1 synapses at SR (Wu and Leung 2003).

The transition from the normal state to epileptiform afterdischarges was accompanied with strong depolarizing waves and increased population excitatory postsynaptic potentials initiating the afterdischarge. The emergence of this depolarizing wave was stimulation site

independent. Our observations are in accordance with Somjen et al. (1985), Buzsaki et al. (1989), Wadman et al. (1992), and Bracci et al. (2001). In addition, there was an early gamma discharge similar to the gamma activation of local circuits of the hippocampus previously described by (Finnerty and Connors 2000). An excessive glutamatergic activation of the hippocampal neuronal network has been shown to result in ultra-synchronous gamma oscillation leading to epileptiform afterdischarges (Medvedev 2001). In conjunction, synchronous activation of inhibitory synapses at gamma frequency has been shown to accumulate chloride into pyramidal cells, thus reducing the efficacy of inhibitory potentials (Bracci et al. 2001). Similar reduction of inhibitory potentials was observable in the increased SR sinks in our CSD data during the epileptiform afterdischarge. Such conditions may aid the afterdischarge generation by challenging the inhibitory neuronal network.

Following the depolarizing wave we recorded a prevalent 10-20 s stable 21 (±2) Hz beta frequency phase in the afterdischarge. Occasionally the network skipped a cycle resulting in 10 Hz beta discharges present in the time-frequency and autocorrelation analyses. The possible mechanisms underlying epileptiform beta frequencies are elusive (Miller 1989; Pare et al. 1992; Charpak et al. 1995; Bracci et al. 1999; Traub et al. 1999b; Jefferys 2003). In our experiment, the synaptic propagation from DG to CA1 *via* CA3 was replaced by nearly simultaneous discharges at DG and CA1. These nearly synchronous discharges were initiated either in DG or CA1. Such non-sequential oscillation suggests the emergence of coupled oscillators (Finnerty and Jefferys 2002; Jefferys 2003). Formation of local oscillators is further supported by the fact that the beta burst stimulation increased and spread the CA1 dendritic excitation in favor of more distal portions of the apical dendritic tree (Wu and Leung 2003). The afterdischarge was terminated at gamma frequencies as described in Bragin et al. (1997), Penttonen et al. (1999), and Ma and Leung (2002).

The early gamma frequency burst coincided with synaptic propagation of the population spikes, whereas the steady-state beta afterdischarges were composed of individual but nearly synchronous population spikes. Furthermore, the autocorrelation analysis omitting the first two seconds of the afterdischarge revealed reduced levels of gamma and theta frequencies. This suggests that the observed epileptiform gamma and beta oscillations represent two distinct oscillatory states that cannot coexist (Penttonen and Buzsaki 2003). Correspondingly, Fellous and Sejnowski (2000) demonstrated that carbachol induced theta and delta oscillations were mutually exclusive. It may be that the observed episodes of gamma frequency activity represent transition phases bordering the actual epileptiform afterdischarge at beta frequencies.

The beta burst stimulation induced a large sink in basal CA1 dendrites. Additionally, the 200 Hz high frequency activity present in the CA1 autocorrelation analysis was missing from the coherence analysis between CA1 and DG indicating that the high frequency activity was restricted to CA1 area. Both basal CA1 dendritic activation and the appearance of fast 200 Hz discharges coincided with the initiation of the epileptiform afterdischarge. This indicates that the recurrent CA1 basal dendritic activation could participate in the local 200 Hz rhythm in

CA1 subfield by recurrent excitation or dendritic backpropagation. The varying amplitudes of the high frequency discharges, on the other hand, suggest that multiple small aggregates fire at an attempt to synchronize themselves prior to the beta frequency transformation (Bikson et al. 2003). Increased beta frequency activity may be the result of increased afterhyperpolarization associated with accumulation of extracellular potassium (Traub et al. 1999b). Such accumulation could aid the formation of coupled oscillators in hippocampal subfields (Jefferys 2003). Pare et al. (1992), and Barbarosie and Avoli (1997) have reported synchronous delta frequency discharges in entorhinal cortex and hippocampus. This suggests that the delta rhythm may involve larger partially extrahippocampal coupled oscillators. This could explain the differential delta wave patterns during perforant path and fimbria-fornix stimulations present in Fig. 3.2. Furthermore, the response frequencies reported in this paper for hippocampal afterdischarges (200, 20, 2 Hz) have been shown to optimally induce long-term potentiation in deep layers of the entorhinal cortex (Yun et al. 2002).

I demonstrate in this chapter that *in vivo* beta burst stimulation induces epileptiform afterdischarges peaking at 200, 20, and 2 Hz with a prominent beta frequency component. These afterdischarges are initiated and terminated at gamma frequencies. We propose that these frequencies correspond to coupling of the epileptiform discharge at different spatial extents or neuronal distances. Hippocampal subfield specific discharges exploit 150-250 Hz high frequencies, intrahippocampal coupled oscillators are formed at 10-30 Hz beta frequencies and 1-2 Hz delta frequencies recruit neuronal components outside the hippocampus. Similar dependency between frequency and cortical distance has been described previously in a model of oscillatory cortical circuits by (Pinto et al. 2003). Such coupled oscillators that are inversely nested in size and frequency could explain the synchronicity at multiple levels of neuronal networks observed during epilepsy.

Chapter 4
Contribution of a single CA3 neuron to network synchrony

Oscillations at theta (3-8 Hz) and gamma (30-80 Hz) frequencies co-occur during arousal, exploration, and rapid eye movement sleep and relate to information processing underlying learning and memory within neuronal networks. In hippocampus, gamma and theta frequency oscillations are associated with modification of synaptic weights, spatial learning, and short-term memory. These oscillations are referred to as network phenomena and, thereby, the role of single neuron oscillations in the generation of functional neuronal networks remains unclear. This chapter demonstrates that an individual CA3 pyramidal cell can activate the CA1 neuronal network in vivo in rat hippocampus using electrical stimulations with simultaneous intracellular gamma and extracellular theta and slow (0.5-1 Hz) frequencies. These results suggest that an individual pyramidal cell can contribute to self-organization of a neuronal small-scale network.

4.1 Introduction

Gamma and theta frequencies have been shown to influence functional neuronal network formation in the living brain (O'Keefe and Recce 1993; Chrobak and Buzsaki 1998b; Engel et al. 2001; Jensen and Lisman 2005). The co-occurrence of these frequencies in the awake brain indicates a period of increased attention to the surrounding environment (Chrobak and Buzsaki 1998b). In conjunction, sleep state gamma and theta oscillations parallel with REM sleep (Cantero et al. 2003). Thereby, these frequencies coincide with brain states that promote cognitive processes such as learning (Wallenstein and Hasselmo 1997), memory (Herrmann et al. 2004; Jensen and Lisman 2005), and binding (Engel et al. 2001; Nowak et al. 1997). Hippocampal gamma and theta frequencies have been mainly encompassed with learning and memory (O'Keefe and Recce 1993; Lisman and Idiart 1995; Mikkonen et al. 2002; Kobayashi and Poo 2004; Jensen and Lisman 2005). Hippocampal gamma rhythm reflects the underlying local interneuronal network rhythm (Penttonen et al. 1998), which is stabilized by pyramidal connections (Chrobak and Buzsaki 1998b) and electrical coupling (Connors and Long 2004; Cunningham et al. 2004). In contrast, theta oscillations are associated with cholinergic and GABAergic neurons of the medial septum (Dragoi et al. 1999) and serotonergic neurons of the Raphe nucleus (Freund et al. 1990), and are thereby mainly extrahippocampal in origin.

Hippocampus has been shown to have intrinsic mechanisms that limit interregional transmission of single action potentials, but allow repeated action potentials to cross subfields (Henze et al. 2002). Additionally, during blockade of GABAergic inhibition *in vitro*, the activity of a few cortical neurons has been shown to recruit the whole population into a coherent oscillation (Wong et al. 1984). Similar recruitment can be achieved also with hippocampal gamma frequency field stimulations that induce timed recurrent activity in the CA3 (Fujisawa et al. 2004) and CA1 (Lisman and Idiart 1995) networks. Here we move forward from these findings to demonstrate that appropriately timed action potentials of a

single CA3 pyramidal cell are followed by similarly timed population responses in CA1 indicating formation of a CA3 to CA1 small-scale neuronal network in hippocampus in vivo.

4.2 Methods

The methods used in the experiments follow the international guidelines on the ethical use of experimental animals and were approved by the State Provincial Office of Eastern Finland (approval number 99-61). The experiments were designed and constructed in order to minimize the number of animals used and their suffering.

4.2.1 Surgical procedures

Experiments were conducted on 17 Kuopio Wistar rats (250-350 g) anesthetized with 1.1-1.4 g/kg urethane. Single Ø60 μm tungsten wire was used for extracellular field potential recording. Extracellular electrode was placed in CA1 pyramidal layer -3.6 mm anteroposterior and -4.0 mm mediolateral from bregma at a 30° angle. Micropipette for intracellular recording (resistance 80-120 MΩ) was pulled from 1 mm filamented quartz capillary glass (P2000 Sutter Instruments, Novato, CA, USA) and filled with 3 M potassium acetate. Intracellular electrode was positioned -3.6 mm anteroposterior and -2.2 mm mediolateral from bregma. Vertical positioning of the extracellular recording electrode was estimated from the polarity of the field response, the shape and firing patterns of the extracellularly evoked compound action potentials (CAPs), and from the latency of the evoked field response. Intracellular electrode was positioned according to temporal cues from the stimulations. Typically, the tips of CA1 and CA3 electrodes were located -2.0 ± 0.2 mm and -2.9 ± 0.2 mm below the cortical surface, respectively. Only neurons with overshooting action potentials and a resting membrane potential below -60 mV were accepted into the analyses. Two stainless steel watch screws, driven into the bone above the cerebellum served as indifferent and ground electrodes in the extracellular recordings, whereas a single subcutaneous chlorinated silver wire was used as the indifferent electrode for intracellular recordings. The intracellular signal was tenfold amplified using an Axoclamp 2B amplifier (Axon Instruments, Foster City, CA, USA), then further fourfold amplified with a Cyberamp380 (Axon Instruments). The EEG signal was 1000-fold amplified using a custom-made amplifier. Thereafter, both signals were low-pass filtered at 6 kHz (Cyberamp380), and finally sampled with 16-bit precision at 10 kHz (Digidata 1320A, Axon Instruments).

4.2.2 Stimulations

Pair of stainless steel wires (100 μm in diameter) with 0.2-0.4 mm tip separation was placed in the fimbria-fornix (-1.3 mm anteroposterior and +1.0 mm mediolateral to bregma; and -4.0 mm ventral from cortical brain surface) to stimulate commissural afferents to the contralateral CA3 region. The intensity of the extracellular 0.2 ms electrical pulse stimulation (Master8 pulse generator and Iso-flex stimulus isolator, A.M.P.I, Jerusalem, Israel) was twice the threshold capable of inducing CAPs in more than two consecutive trials. The stimulation intensity was between 140 and 300 μA. The pathway of the stimulation (fimbria-fornix -> CA3 -> CA1) was confirmed by simultaneous intra- and extracellular recordings from CA3 and CA1. This included monitoring of the temporal order of CA3 action potentials and CA1

CAPs. Intracellular stimulations were current injections through the intracellular electrode. In these stimulations, the Master8 pulse generator triggered Axoclamp 2B amplifier to deliver 2 ms current pulses at +0.5 - +1.0 nA.

We used stimulation patterns with naturally co-occurring gamma, theta and slow frequencies (Mikkonen et al. 2002; Penttonen and Buzsaki 2003). Intracellular stimulations consisted of four intracellular gamma frequency pulses repeating four times at theta intervals. Gamma frequencies were either 40 or 60 Hz. Similarly, the underlying theta frequency was either 4 or 6 Hz maintaining the gamma/theta ratio at 10. The four theta cycles further repeated at 0.5 Hz slow frequency intervals. Therefore, the stimulation consisted of three different interleaved stimulation frequencies: gamma, theta and slow. Due to hardware configuration, extracellular theta stimulation preceded intracellular theta stimulation by 3 ms. Stimulations consisted of three 10 s periods: intracellular gamma frequency stimulation (IS), extracellular theta frequency stimulation (ES) or combined intracellular gamma and extracellular theta frequency stimulation (IES). The order of the periods varied randomly. In each stimulation period, stimulation frequencies were kept constant.

4.2.3 Data analyses

CAPs were determined as local field fluctuations that exceeded 1 mV in peak to peak amplitude and returned to baseline. Instantaneous frequency was calculated as the interval between the negative (extracellular) and positive (intracellular) peaks of two consecutive induced CAPs or action potentials, respectively. Chi squared -test was used for estimations of prevalence differences on data pooled from the responsive animals. The inter-spike interval data was then divided into groups corresponding to different stimulation periods at different frequencies. Temporal evolution of the stimulation cycles was analyzed using repeated measures analysis of variance (ANOVA). Two-way ANOVA with Bonferroni corrected least significant differences -test for pair-wise comparisons was used to analyze differences between ES, and IES at different stimulation frequencies. Spectral densities were calculated and averaged for extracellular CA1 data. The mean densities were obtained from the first and the last 2 s of the stimulation, *i.e.* the first and the last slow stimulation cycle, without filtering. Results were normalized between 25-120 Hz using Matlab (MathWorks Inc, Natick, MA, USA). Subsequently the gamma frequency differences between different stimulation times and conditions were analyzed for the first and the last slow 0.5 Hz cycle. Finally, paired Student's T -test was used for pair-wise comparisons and results were individually plotted to aid interpretation of the results.

4.3 Results

We investigated the generation of cellular ensembles in rat hippocampus in vivo using multiple coexisting oscillation patterns (Penttonen and Buzsaki 2003): intracellular stimulations at gamma, theta and slow frequencies and concurrent extracellular stimulations at theta and slow frequencies. In essence, we combined intracellular CA3 gamma stimulation with extrahippocampal theta stimulation in order to create "local" fast gamma oscillations with "global" theta oscillations in the background (Buzsaki and Draguhn 2004). Our four-

pulse intracellular CA3 stimulation at gamma frequency resulted in a burst of overshooting action potentials, and at the same time, the rest of the hippocampal network was silenced and sensitized by the fimbria fornix stimulation (Figs. 4.1C and 4.1E). This silencing and sensitization result from simultaneous large-scale activation of the interneuronal network and resetting of the theta oscillation with septal origin (Dragoi et al. 1999; Zugaro et al. 2005). We recorded intracellularly 34 CA3 pyramidal cells from 17 Kuopio Wistar rats with concurrent extracellular recordings from CA1 to isolate CA1 local field oscillations as compound action potentials (CAPs). Regardless of the fact that blind insertion of extra- and intracellular electrodes in vivo seldom targets a connection between a CA3 pyramidal cell and an ensemble of neurons generating the measured local field in CA1, we managed to have a CA3-CA1 connection that resulted in CAPs in 44 % of the animals and 32 % of the neurons. The high percentage is likely due to the interconnected CA3 neuronal network activating more than the single CA3 pyramidal cell in response to the intracellular stimulation.

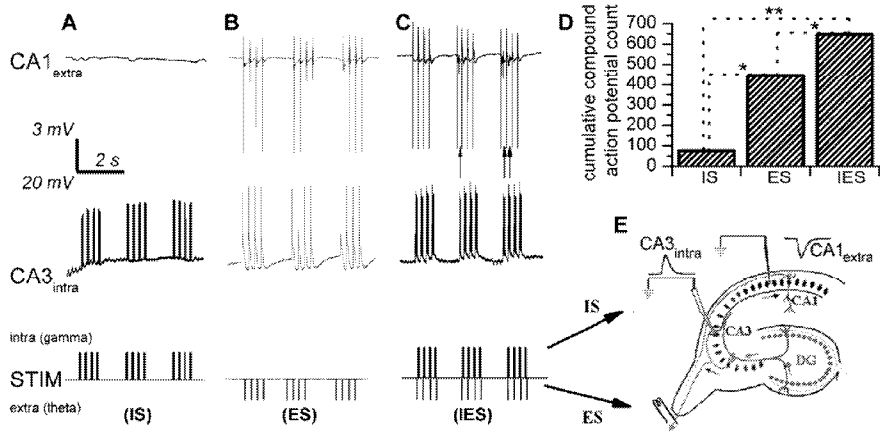

Fig. 4.1 Combined intracellular CA3 gamma and extracellular fimbria fornix theta frequency stimulation induce compound action potentials (CAPs) in CA1. **A)** Intracellular CA3 stimulation (IS). **B)** Extracellular fimbria fornix stimulation (ES). **C)** Combined intracellular and extracellular stimulation (IES). Traces in subfigures here and in subsequent figures: extracellular CA1 recording (CA1extra), intracellular CA3 recording (CA3intra), and stimulations (STIM). Note that intracellular recordings include four pulses at gamma frequency identifiable as intensified black color. Note also the difference between stimulation evoked CAPs vertically aligned to stimulations (the 10 mV deflections in **B** and **C**) and induced CA1 CAPs (vertical arrows). **D)** Summed total CAP count from all animals induced by different stimulations ($\chi 2$ - test, * $p < 0.05$ and ** $p < 0.01$). **E)** Stimulation design demonstrating recording and stimulation sites. Arrows indicate the locations of IS and ES. Note that intracellular CA3 recording and stimulation occurs with the same electrode.

4.3.1 Development of intracellularly induced CA1 CAPs

To address the possibility that these CA1 CAPs had been generated by "local" intracellular or "global" extracellular stimulation alone, we examined the activity of CA1 neuronal network

following only intracellular stimulation (IS) and only extracellular stimulation (ES) in addition to combined intra- and extracellular stimulation (IES, Fig. 4.1). In other words, our experimental paradigm consisted of two internal controls: gamma-theta-slow frequency CA3 IS (Fig. 4.1A) and fimbria-fornix theta-slow frequency ES (Fig. 4.1B). We detected CAPs in CA1 after 5% of the IS. ES, on the other hand, induced CAPs in CA1 in 21 % of the stimulations. However, IES was significantly the most potent activator of the CA1 network, as 37 % of the stimulations yielded CAPs in CA1 (Fig. 4.1D).

Examination of the temporal evolution of the IES induced changes in the CA3-CA1 network revealed generation of CAPs in CA1 during repetition of the cyclic stimulation. As evidenced in Figure 4.2, the first slow cycle with the IES had little if any effect on the network behavior. However, the repetition of the slow cycle with embedded gamma-theta stimulation significantly increased the number of CAPs in CA1 (Figs. 4.2A-C). Similar potentiation of the CAP induction was not present in ES, but the network had an unaltered field response to ES throughout the repetitions of the fimbria-fornix stimulation (Fig. 4.2C). It is noteworthy that the temporal window between the first fimbria-fornix and CA3 stimulation pulses and the first induced synchronized CA1 CAP was in order of seconds, i.e. in the next slow cycle. The two second (0.5 Hz) cyclic time delay observed here relates to evoked synchronized CA3 burst delay (Staley et al. 2001) and alteration of up and down states within cortical neuronal networks (Cossart et al. 2003).

4.3.2 Intracellular CA3 stimulation and the frequency of the CA1 network CAPs

We determined the influence of stimulation frequency on the induced CA1 CAPs using ES at 4 and 6 Hz and IES at 40/4 and 60/6 Hz. In other words, we created two comparable situations for two frequencies, which differed only by the presence of the intracellular gamma stimulation. Both ES and IES induced gamma field effects in CA1. In order to quantify the results we pooled the results from all the recorded neurons from the responsive animals and compared the prevalence of stimulation induced CAPs in the CA1 network. Neither the total frequency content between 60/6 and 40/4 Hz IES nor 6 and 4 Hz ES stimulations differed significantly. Since we were interested in the gamma frequency range and low frequencies dominated the overall frequency count, we adjusted the analysis by selecting only the gamma frequency CAPs (N = 139). This selection yielded significantly different results in the IES, but not in the ES groups (Fig. 4.3A). The ES gamma CAPs had mean (± s.e.m.) frequencies of 45 ± 4 Hz (ES 6 Hz) and 42 ± 5 Hz (ES 4 Hz). IES gamma CAP means were 50 ± 3 Hz (IES 60/6 Hz) and 41 ± 2 Hz (IES 40/4 Hz). These findings are in parallel with previous research where CA1 has been shown to retain the periodicity of induced gamma frequency patterns in vivo (Mikkonen et al. 2002). However, our current results demonstrate that instead of an extracellular "global" stimulation, a single CA3 cell can act as a "local" pacemaker for cellular ensembles in CA1.

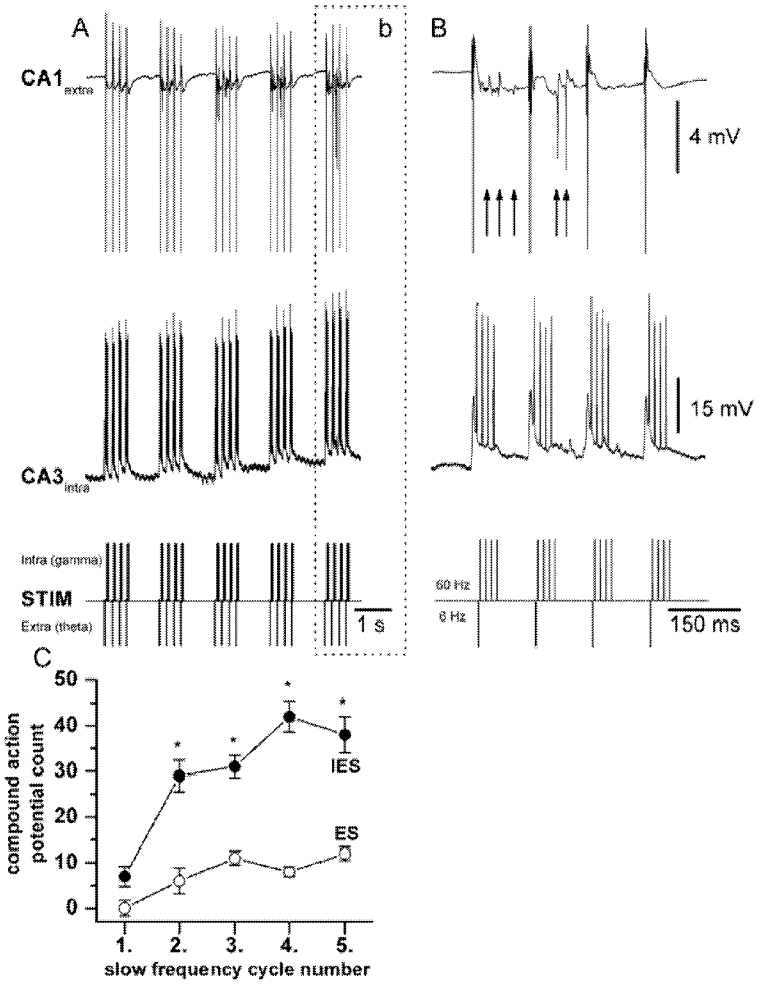

Fig. 4.2 Temporal evolution of the combined CA3 intracellular and fimbria fornix extracellular stimulation (IES) induced CA1 compound action potentials (CAPs). **A)** Complete IES with 60 Hz gamma, 6 Hz theta, and 0.5 Hz slow frequencies. **B)** Magnification of the final theta cycles in **A**. Vertical arrows indicate induced CA1 CAPs. **C)** CAPs as a function of stimulation time for IES and extracellular stimulation (ES). Horizontal axis shows the slow frequency cycles. Note the increase of CAPs (± s.e.m.) in IES and the steady state response in ES (repeated measures ANOVA, * $p < 0.02$, $N_{cycle} = 8$ and $p < 0.015$, $N_{IES\_vs\_ES} = 40$).

We next investigated IES (40/4 and 60/6 Hz) and ES (4 and 6 Hz) repetition induced temporal changes in the CAP mean (N = 5 for each stimulation frequency) gamma frequency content in CA1 by comparing spectral densities during the first and the last 2 s of the stimulation (Fig. 4.3B). In IES, the gamma power increased as a function of stimulation time. The peak frequencies of this increase reflected the IES gamma frequency. In contrast, ES had no systematic effect on the CA1 gamma power between the first and last two seconds of the

stimulation. Furthermore, there were no differences in theta frequencies between IES and ES (data not shown). Since the only difference between the stimulation conditions was the intracellular CA3 pyramidal cell gamma stimulation in IES, these results indicate enhanced efficacy of gamma frequency synaptic transmission in IES, but not in ES. Thereby our results emphasize the specific role of individual neurons working at gamma frequencies (Henze et al. 2002; Csicsvari et al. 2003), yet responding to multiple coexisting spike patterns (Penttonen and Buzsaki 2003; Buzsaki and Draguhn 2004), in neuronal networks.

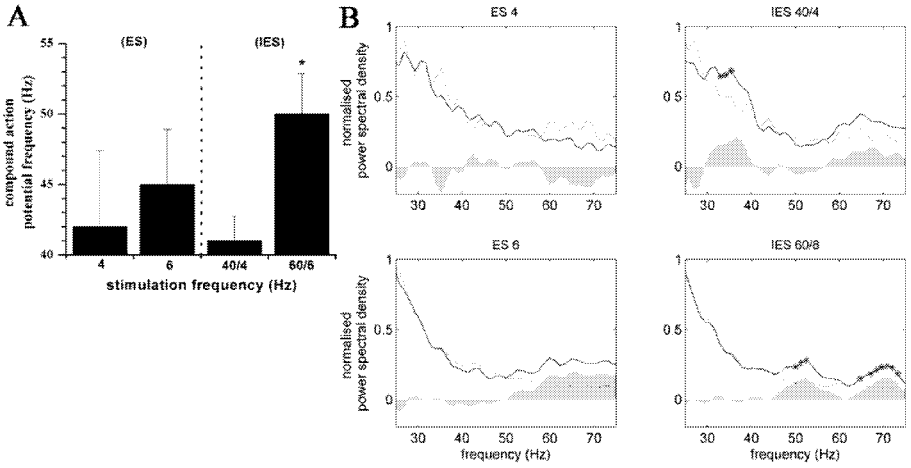

Fig. 4.3 CA1 field gamma frequencies are changed intracellular stimulation frequency dependently following combined CA3 intracellular and fimbria-fornix extracellular stimulation (IES). **A)** Instantaneous frequencies (± s.e.m.) from 12 neurons showing CA1 compound action potentials during extracellular stimulation (ES) at 4 and 6 Hz and IES at 40/4 and 60/6 Hz (2-way ANOVA, * $p < 0.05$). **B)** Temporal evolution of mean ($N = 5$ for each stimulation frequency) power spectral densities during IES and ES. Lines represent the normalized densities in response to first (dashed) and last (solid) stimulation cycles. Grey contour demonstrates the difference between the cycles (paired T -test, * $p < 0.05$).

4.4 Discussion

IES and ES evoked CA1 theta frequency CAPs time-locked to the stimulation. This indicates that our stimulation was successful in creating a rhythmic activity in the theta band across the hippocampal neuronal network (Dragoi et al. 1999). The induced theta drive resembles also the theta-burst stimulation protocol typically used in long-term potentiation studies (Nguyen and Kandel 1997). The external theta frequency drive was necessary for the observed CA3 and CA1 events since the induced theta frequency forced the hippocampal neuronal network into a sensitized state (Mikkonen et al. 2002; Zugaro et al. 2005) and maintained the network in that state. The local gamma oscillations emerged only on that steady theta rhythm. This indicates that more widely spread theta frequencies may be considered as a prerequisite for local hippocampal gamma frequencies (Buzsaki and Draguhn 2004) and that different frequency ranges serve different, partially overlapping, functions within intact neuronal

networks (Steriade 2001). Even the sole extracellular theta stimulation driven experiments were therefore able to benefit from the suitable network conditions and generated CAPs in the CA1. However, the number of incidences and, more importantly, the gamma power of these multiunit events were low. Conversely, the combined intracellular and extracellular stimulation driven experiments benefited from both the external theta drive and the local gamma pacemaker, thus forming coherent theta and gamma frequency CAPs in the CA1 multiunit activity. The fimbria-fornix stimulation further enhanced the induced gamma by removing CAP frequency adaptation from CA1 pyramidal neurons (Penttonen et al. 1998). Furthermore, the emergence of the CA1 CAPs required repetition at slow frequency. This may represent the hippocampal form of neocortical up and down states (Cossart et al. 2003; Battaglia et al. 2004) thus clarifying the temporal requirements of the CA3 pyramidal cell interactions in signal transmission.

We suggest that after the extracellular theta stimulation the emergence of network activity was based on random initiation: any of the CA3 neurons might have initiated the oscillation at any gamma frequency thereby inducing a variable oscillation. The ES activated the CA3 recurrent collaterals that stimulated the CA1 network into firing threshold, but there was no preferential gamma frequency drive in the network that could have facilitated the emergence of coherent gamma frequency oscillations (Buzsaki and Draguhn 2004). The IES, in contrast, pre-selected the neuron that would activate the network. Thereby the stimulated neuron acted as a pacemaker that mostly contributed to the formation of a neuronal ensemble in CA3-CA1 neuronal network. This way, a single electrically stimulated CA3 pyramidal cell was sufficient in generating the CA1 CAP response. Single cell induced activation of a "pre-wired" functional neuronal network has been previously reported in rat motor cortex (Brecht et al. 2004). In our experiment, the activated network was generated by intracellular gamma frequency stimulation of a randomly chosen CA3 neuron and, furthermore, the IES at 40 and 60 Hz yielded synchronous gamma stimulation frequency dependent CAPs in CA1 neuronal network. Although these frequency dependent responses might emerge from distinct populations of neurons in the CA1 neuronal network (Izhikevich et al. 2003), the CA1 neuronal population response to the single CA3 pyramidal cell input suggests that in vivo neuronal network can self organize to meet the demands of its inputs (Buzsaki and Draguhn 2004). Our results may provide new insight into self-organization principles of natural neuronal networks.

Chapter 5
Concluding remarks

The scope of this dissertation has been to investigate the time varying nature and properties of different fast frequency oscillations in hippocampus. Based on the results it seems that the fast frequencies can be integrated into a single core hypothesis where gamma and theta frequencies are required to induce self-sustaining changes in temporal network dynamics, whereas beta and delta frequencies cannot alter normal network dynamics. In contrast, attempts to induce network connectivity changes at beta and delta frequencies transformed the hippocampal neuronal network into an epileptiform uncontrolled bursting state. Additionally, gamma frequencies are locally generated and single neurons operating at gamma frequencies can contribute to assembly formation. These local gamma frequency induced changes must, however, be accompanied by a correct network state that enables the gamma frequencies to pass cellular subfields. Such network state seems to be in a rhythmic state in the theta band. As reported earlier by Jensen and Lisman (1998), these novel patterns must repeat until they are recognized as acceptable network structures.

The frequency bands follow a simple rule that eliminates cross-talk between oscillation frequencies: neighboring frequency bands cannot be active at the same time. This was evident in chapter 3, where increased autocorrelation at fast, beta, and delta frequencies was accompanied with a decrease at gamma and theta frequencies. Additionally, the reverse relationship between increasing frequency and spatial scale was revealed: local groups were acting at 200 Hz and hippocampal oscillators at 20 Hz, whereas the source for 2 Hz frequency synchronization could not be determined with sole intrahippocampal recordings. Self-sustaining alterations of the brain rhythms at different frequencies promote self organization of functional neuronal networks and may provide the foundations for learning and memory. Oscillatory organization would be a rapid and energetically efficient solution to represent the universal abstractions from the environment. This view is supported by the evolutionary stableness of the brain rhythms (Penttonen and Buzsaki 2003).

5.1 Future directions

This dissertation has opened new lines for further investigations. For example, we should use refined correlation and clustering analyses of separate neuronal ensembles in order to discover the role of different frequencies in the synchronization and desynchronization of the network. In addition, independent component analysis should be used to identify smaller sub-ensembles of neurons from larger groups. Multielectrode recordings from hippocampus and its target structures using the above mentioned techniques could reveal the temporal and frequency band integration of the neuronal circuitry. Furthermore, functional magnetic resonance imaging could identify large neuronal groups operating at low frequencies. Eventually, behavioral measurements and comparisons of oscillations at different frequencies during normal behavior and standard learning paradigms should be performed.

Reference list

Amaral, D. G. and Witter, M. P. The three-dimensional organization of the hippocampal formation: a review of anatomical data. Neuroscience 31: 571-91, 1989.

Amaral, D. G., and Witter, M. P. Hippocampal formation. In: The rat nervous system, 2nd ed, Paxinos, G. ed., San Diego: Academic Press 443-93, 1995

Amzica, F. and Steriade, M. Spontaneous and artificial activation of neocortical seizures. J Neurophysiol 82: 3123-38, 1999.

Babb, T. L. and Brown, W. J. Pathological findings in epilepsy. New York: Raven Press. 511-40, 1987.

Barbarosie, M. and Avoli, M. CA3-driven hippocampal-entorhinal loop controls rather than sustains in vitro limbic seizures. J Neurosci 17: 9308-14, 1997.

Battaglia, F. P., Sutherland, G. R., and McNaughton, B. L. Hippocampal sharp wave bursts coincide with neocortical "up-state" transitions. Learn Mem 11: 697-704, 2004.

Bernard, C. and Wheal, H. V. Model of local connectivity patterns in CA3 and CA1 areas of the hippocampus. Hippocampus 4: 497-529, 1994.

Bi, G. Q. and Poo, M. M. Synaptic modifications in cultured hippocampal neurons: dependence on spike timing, synaptic strength, and postsynaptic cell type. J Neurosci 18: 10464-72, 1998.

Bikson, M., Fox, J. E., and Jefferys, J. G. Neuronal aggregate formation underlies spatiotemporal dynamics of nonsynaptic seizure initiation. J Neurophysiol 89: 2330-3, 2003.

Bland, B. H. The physiology and pharmacology of hippocampal formation theta rhythms. Prog Neurobiol 26: 1-54, 1986.

Bracci, E., Vreugdenhil, M., Hack, S. P., and Jefferys, J. G. On the synchronizing mechanisms of tetanically induced hippocampal oscillations. J Neurosci 19: 8104-13, 1999.

Bracci, E., Vreugdenhil, M., Hack, S. P., and Jefferys, J. G. Dynamic modulation of excitation and inhibition during stimulation at gamma and beta frequencies in the CA1 hippocampal region. J Neurophysiol 85: 2412-22, 2001.

Bragin, A., Csicsvari, J., Penttonen, M., and Buzsaki, G. Epileptic afterdischarge in the hippocampal-entorhinal system: current source density and unit studies. Neuroscience 76: 1187-203, 1997.

Bragin, A., Jando, G., Nadasdy, Z., Hetke, J., Wise, K., and Buzsaki, G. Gamma (40-100 Hz) oscillation in the hippocampus of the behaving rat. J Neurosci 15: 47-60, 1995.

Bragin, A., Mody, I., Wilson, C. L., and Engel, J. Jr Local generation of fast ripples in epileptic brain. J Neurosci 22: 2012-21, 2002.

Bragin, A., Penttonen, M., and Buzsaki, G. Termination of epileptic afterdischarge in the hippocampus. J Neurosci 17: 2567-79, 1997.

Brecht, M., Schneider, M., Sakmann, B., and Margrie, T. W. Whisker movements evoked by stimulation of single pyramidal cells in rat motor cortex. Nature 427: 704-10, 2004.

Buzsaki, G. Two-stage model of memory trace formation: a role for "noisy" brain states. Neuroscience 31: 551-70, 1989.

Buzsaki, G. Theta oscillations in the hippocampus. Neuron 33: 325-40, 2002.

Buzsaki, G. and Chrobak, J. J. Temporal structure in spatially organized neuronal ensembles: a role for interneuronal networks. Curr Opin Neurobiol 5: 504-10, 1995.

Buzsaki, G. and Draguhn, A. Neuronal oscillations in cortical networks. Science 304: 1926-9, 2004.

Buzsaki, G., Leung, L. W., and Vanderwolf, C. H. Cellular bases of hippocampal EEG in the behaving rat. Brain Res 287: 139-71, 1983.

Buzsaki, G., Ponomareff, G. L., Bayardo, F., Ruiz, R., and Gage, F. H. Neuronal activity in the subcortically denervated hippocampus: a chronic model for epilepsy. Neuroscience 28: 527-38, 1989.

Cantero, J. L., Atienza, M., Stickgold, R., Kahana, M. J., Madsen, J. R., and Kocsis, B. Sleep-dependent theta oscillations in the human hippocampus and neocortex. J Neurosci 23: 10897-903, 2003.

Caton, R. The electric currents of the brain. Br. Med. J. 2: 278, 1875.

Cavazos, J. E., Das, I., and Sutula, T. P. Neuronal loss induced in limbic pathways by kindling: evidence for induction of hippocampal sclerosis by repeated brief seizures. J Neurosci 14: 3106-21, 1994.

Charpak, S., Pare, D., and Llinas, R. The entorhinal cortex entrains fast CA1 hippocampal oscillations in the anaesthetized guinea-pig: role of the monosynaptic component of the perforant path. Eur J Neurosci 7: 1548-57, 1995.

Chrobak, J. J. and Buzsaki, G. Gamma oscillations in the entorhinal cortex of the freely behaving rat. J Neurosci 18: 388-98, 1998a.

Chrobak, J. J. and Buzsaki, G. Operational dynamics in the hippocampal-entorhinal axis. Neurosci Biobehav Rev 22: 303-10, 1998b.

Connors, B. W. and Long, M. A. Electrical synapses in the mammalian brain. Annu Rev Neurosci 27: 393-418, 2004.

Contreras, D. and Steriade, M. Cellular basis of EEG slow rhythms: a study of dynamic corticothalamic relationships. J Neurosci 15: 604-22, 1995.

Contreras, D., Timofeev, I., and Steriade, M. Mechanisms of long-lasting hyperpolarizations underlying slow sleep oscillations in cat corticothalamic networks. J Physiol 494: 251-64, 1996.

Cossart, R., Aronov, D., and Yuste, R. Attractor dynamics of network UP states in the neocortex. Nature 423: 283-8, 2003.

Csicsvari, J., Hirase, H., Mamiya, A., and Buzsaki, G. Ensemble patterns of hippocampal CA3-CA1 neurons during sharp wave- associated population events. Neuron 28: 585-94, 2000.

Csicsvari, J., Jamieson, B., Wise, K. D., and Buzsaki, G. Mechanisms of gamma oscillations in the hippocampus of the behaving rat. Neuron 37: 311-22, 2003.

Cunningham, M. O., Whittington, M. A., Bibbig, A., Roopun, A., LeBeau, F. E., Vogt, A., Monyer, H., Buhl, E. H., and Traub, R. D. A role for fast rhythmic bursting neurons in cortical gamma oscillations in vitro. Proc Natl Acad Sci USA 101: 7152-7, 2004.

DeFelipe, J. and Jones, E. G. Santiago Ramon y Cajal and methods in neurohistology. Trends Neurosci 15: 237-46, 1992.

Doheny, H. C., Faulkner, H. J., Gruzelier, J. H., Baldeweg, T., and Whittington, M. A. Pathway-specific habituation of induced gamma oscillations in the hippocampal slice. Neuroreport 11: 2629-33, 2000.

Dragoi, G., Carpi, D., Recce, M., Csicsvari, J., and Buzsaki, G. Interactions between hippocampus and medial septum during sharp waves and theta oscillation in the behaving rat. J Neurosci 19: 6191-9, 1999.

Draguhn, A., Traub, R. D., Bibbig, A., and Schmitz, D. Ripple (approximately 200-Hz) oscillations in temporal structures. J Clin Neurophysiol 17: 361-76, 2000.

Eichenbaum, H. A cortical-hippocampal system for declarative memory. Nat Rev Neurosci 1: 41-50, 2000.

Engel A. K. , Fries P. , and Singer W. Dynamic predictions: Oscillations and synchrony in top-down processing. Nat Rev Neurosci 2: 704-16, 2001.

Evans, M. S., Viola-McCabe, K. E., Caspary, D. M., and Faingold, C. L. Loss of synaptic inhibition during repetitive stimulation in genetically epilepsy-prone rats (GEPR). Epilepsy Res 18: 97-105, 1994.

Fellous, J. M. and Sejnowski, T. J. Cholinergic induction of oscillations in the hippocampal slice in the slow (0.5-2 Hz), theta (5-12 Hz), and gamma (35-70 Hz) bands. Hippocampus 10: 187-97, 2000.

Finnerty, G. T. and Connors, B. W. Sensory deprivation without competition yields modest alterations of short-term synaptic dynamics. Proc Natl Acad Sci USA 97: 12864-8, 2000.

Finnerty, G. T. and Jefferys, J. G. Investigation of the neuronal aggregate generating seizures in the rat tetanus toxin model of epilepsy. J Neurophysiol 88: 2919-27, 2002.

Fisahn, A., Pike, F. G., Buhl, E. H., and Paulsen, O. Cholinergic induction of network oscillations at 40 Hz in the hippocampus in vitro. Nature 394: 186-9, 1998.

Freeman, J. A. and Nicholson, C. Experimental optimization of current source-density technique for anuran cerebellum. J Neurophysiol 38: 369-82, 1975.

Freund, T. F. and Buzsaki, G. Interneurons of the hippocampus. Hippocampus 6: 347-470, 1996.

Freund, T. F., Gulyas, A. I., Acsady, L., Gorcs, T., and Toth, K. Serotonergic control of the hippocampus via local inhibitory interneurons. Proc Natl Acad Sci USA 87: 8501-5, 1990.

Fricker, D. and Miles, R. EPSP amplification and the precision of spike timing in hippocampal neurons. Neuron 28: 559-69, 2000.

Fujisawa, S., Matsuki, N., and Ikegaya, Y. Chronometric readout from a memory trace: gamma-frequency field stimulation recruits timed recurrent activity in the rat CA3 network. J Physiol 561: 123-31, 2004.

Gloveli, T., Dugladze, T., Saha, S., Monyer, H., Heinemann, U., Traub, R. D., Whittington, M. A., and Buhl, E. H. Differential involvement of oriens/pyramidale interneurones in hippocampal network oscillations in vitro. J Physiol 562: 131-47, 2005.

Gloveli, T., Schmitz, D., Empson, R. M., and Heinemann, U. Frequency-dependent information flow from the entorhinal cortex to the hippocampus. J Neurophysiol 78: 3444-9, 1997.

Gluckman, B. J., Nguyen, H., Weinstein, S. L., and Schiff, S. J. Adaptive electric field control of epileptic seizures. J Neurosci 21: 590-600, 2001.

Golarai, G., Greenwood, A. C., Feeney, D. M., and Connor, J. A. Physiological and structural evidence for hippocampal involvement in persistent seizure susceptibility after traumatic brain injury. J Neurosci 21: 8523-37, 2001.

Gray, C. M. Synchronous oscillations in neuronal systems: mechanisms and functions. J Comput Neurosci 1: 11-38, 1994.

Green, J. D. and Arduni, A. A. Hippocampal electrical activity in arousal. J. Neurophysiol. 17: 533-57, 1954.

Gulyas, A. I., Acsady, L., and Freund, T. F. Structural basis of the cholinergic and serotonergic modulation of GABAergic neurons in the hippocampus. Neurochem Int 34: 359-72, 1999.

Hasselmo, M. E. and Schnell, E. Laminar selectivity of the cholinergic suppression of synaptic transmission in rat hippocampal region CA1: computational modelling and brain slice physiology. J Neurosci 14: 3898-914, 1994.

Hasselmo, M. E., Schnell, E., and Barkai, E. Dynamics of learning and recall at excitatory recurrent synapses and cholinergic modulation in rat hippocampal region CA3. J Neurosci 15: 5249 -62, 1995.

Hebb, D. O. The organization of behavior; a neuropsychological theory. New York, Wiley. 1949.

Heltovics, G., Boda, B., and Szente, M. Anticonvulsive effect of urethane on aminopyridine-induced epileptiform activity. Neuroreport 6: 577-80, 1995.

Henze, D. A., Wittner, L., and Buzsaki, G. Single granule cells reliably discharge targets in the hippocampal CA3 network in vivo. Nat Neurosci 5: 790-5, 2002.

Herrmann, C. S., Munk, M. H., and Engel, A. K. Cognitive functions of gamma-band activity: memory match and utilization. Trends Cogn Sci 8: 347-55, 2004.

Heynen, A. J. and Bear, M. F. Long-term potentiation of thalamocortical transmission in the adult visual cortex in vivo. J Neurosci 21: 9801-13, 2001.

Hirai, N., Uchida, S., Maehara, T., Okubo, Y., and Shimizu, H. Beta-1 (10-20 Hz) cortical oscillations observed in the human medial temporal lobe. Neuroreport 10: 3055-9, 1999.

Holscher, C., Anwyl, R., and Rowan, M. Block of HFS-induced LTP in the dentate gyrus by 1S,3S-ACPD: further evidence against LTP as a model for learning. Neuroreport 8: 451-4, 1997a.

Holscher, C., Anwyl, R., and Rowan, M. J. Stimulation on the positive phase of hippocampal theta rhythm induces long-term potentiation that can Be depotentiated by stimulation on the negative phase in area CA1 in vivo. J Neurosci 17: 6470-7, 1997b.

Holsheimer, J. Electrical conductivity of the hippocampal CA1 layers and application to current-source-density analysis. Exp Brain Res 67: 402-10, 1987.

Huerta, P. T. and Lisman, J. E. Heightened synaptic plasticity of hippocampal CA1 neurons during a

cholinergically induced rhythmic state. Nature 364: 723-5, 1993.

Hyman, J. M., Wyble, B. P., Goyal, V., Rossi, C. A., and Hasselmo, M. E. Stimulation in hippocampal region CA1 in behaving rats yields long-term potentiation when delivered to the peak of theta and long-term depression when delivered to the trough. J Neurosci 23: 11725-31, 2003.

Izhikevich, E. M., Desai, N. S., Walcott, E. C., and Hoppensteadt F. C. Bursts as unit of neural information: selective communication via resonance. Trends Neurosci 26: 161-7, 2003.

Jefferys, J. G. Models and mechanisms of experimental epilepsies. Epilepsia 44 Suppl 12: 44-50, 2003.

Jefferys, J. G., Traub, R. D., and Whittington, M. A. Neuronal networks for induced '40 Hz' rhythms. Trends Neurosci 19: 202-8, 1996.

Jensen, O. and Lisman, J. E. An oscillatory short-term memory buffer model can account for data on the Sternberg task. J Neurosci 18: 10688-99, 1998.

Jensen, O. and Lisman, J. E. Hippocampal sequence-encoding driven by a cortical multi-item working memory buffer. Trends Neurosci 28: 67-72, 2005.

Kahana, M. J., Sekuler, R., Caplan, J. B., Kirschen, M., and Madsen, J. R. Human theta oscillations exhibit task dependence during virtual maze navigation. Nature 399: 781-4, 1999.

Kaibara, T. and Leung, L. S. Basal versus apical dendritic long-term potentiation of commissural afferents to hippocampal CA1: a current-source density study. J Neurosci 13: 2391-404, 1993.

Kloosterman, F., Peloquin, P., and Leung, L. S. Apical and basal orthodromic population spikes in hippocampal CA1 in vivo show different origins and patterns of propagation. J Neurophysiol 86: 2435-44, 2001.

Kobayashi, K. and Poo, M. M. Spike train timing-dependent associative modification of hippocampal CA3 recurrent synapses by mossy fibers. Neuron 41: 445-54, 2004.

Kohling, R., Qu, M., Zilles, K., and Speckmann, E. J. Current-source-density profiles associated with sharp waves in human epileptic neocortical tissue. Neuroscience 94: 1039-50, 1999.

Kolta, A., Ambros-Ingerson, J., and Lynch, G. Early and late components of AMPA-receptor mediated field potentials in hippocampal slices. Brain Res 737: 133-45, 1996.

Liang, H., Bressler, S. L., Ding, M., Truccolo, W. A., and Nakamura, R. Synchronized activity in prefrontal cortex during anticipation of visuomotor processing. Neuroreport 13: 2011-5, 2002.

Lisman, J. E. and Idiart, M. A. Storage of 7 +/- 2 short-term memories in oscillatory subcycles. Science 267: 1512-5, 1995.

Lothman, E. W. and Williamson, J. M. Influence of electrical stimulus parameters on afterdischarge thresholds in the rat hippocampus. Epilepsy Res 13: 205-13, 1992.

Lowenstein, D. H., Thomas, M. J., Smith, D. J., and McIntosh, T. K. Selective vulnerability of dentate hilar neurons following traumatic brain injury: a potential mechanistic link between head trauma and disorders of the hippocampus. J Neurosci 12: 4846-53, 1992.

Ma, J. and Leung, L. S. Metabotropic glutamate receptors in the hippocampus and nucleus accumbens are involved in generating seizure-induced hippocampal gamma waves and behavioral hyperactivity. Behav Brain Res 133: 45-56, 2002.

MacLeod, K., Backer, A., and Laurent, G. Who reads temporal information contained across synchronized and oscillatory spike trains? Nature 395: 693-8, 1998.

Maguire, E. A., Frackowiak, R. S., and Frith, C. D. Recalling routes around london: activation of the right hippocampus in taxi drivers. J Neurosci 17: 7103-10, 1997.

Markram, H., Lubke, J., Frotscher, M., and Sakmann, B. Regulation of synaptic efficacy by coincidence of postsynaptic APs and EPSPs [see comments]. Science 275: 213-5, 1997.

McBain, C. J. and Fisahn, A. Interneurons unbound. Nat Rev Neurosci 2: 11-23, 2001.

McCormick, D. A. and Contreras, D. On the cellular and network bases of epileptic seizures. Annu Rev Physiol 63: 815-46, 2001.

Medvedev, A., Mackenzie, L., Hiscock, J. J., and Willoughby, J. O. Kainic acid induces distinct types of epileptiform discharge with differential involvement of hippocampus and neocortex. Brain Res Bull 52: 89-98,

2000.

Medvedev, A. V. Temporal binding at gamma frequencies in the brain: paving the way to epilepsy? Australas Phys Eng Sci Med 24: 37-48, 2001.

Merriam-Webster online dictionary. January 6th, 2006.

Mikkonen, J. E., Gronfors, T., Chrobak, J. J., and Penttonen, M. Hippocampus retains the periodicity of gamma stimulation in vivo. J Neurophysiol 88: 2349-54, 2002.

Miles, R. and Wong, R. K. Excitatory synaptic interactions between CA3 neurones in the guinea-pig hippocampus. J Physiol 373: 397-418, 1986.

Miller, R. Cortico-hippocampal interplay: Self-organizing phase-locked loops for indexing memory. Psychobiol 17: 115-28, 1989.

Mori, M., Abegg, M. H., Gahwiler, B. H., and Gerber, U. A frequency-dependent switch from inhibition to excitation in a hippocampal unitary circuit. Nature 431: 453-6, 2004.

Morris, R. G. M., Garrud, P., Rawlins, J. N. P., and O'Keefe, J. Place navigation impaired in rats with hippocampal lesions. Nature 297: 681-83, 1982.

Muller, R. U. and Kubie, J. L. The effects of changes in the environment on the spatial firing of hippocampal complex-spike cells. J Neurosci 7: 1951-68, 1987.

Muthuswamy, J. and Thakor, N. V. Spectral analysis methods for neurological signals. J Neurosci Methods 83: 1-14, 1998.

Nguyen, P. V. and Kandel, E. R. Brief theta-burst stimulation induces a transcription-dependent late phase of LTP requiring cAMP in area CA1 of the mouse hippocampus. Learn Mem. 4: 230-43, 1997.

Nowak, L. G., Sanchez-Vives, M. V., and McCormick, D. A. Influence of low and high frequency inputs on spike timing in visual cortical neurons. Cereb Cortex 7: 487-501, 1997.

O'Keefe, J. and Nadel, L. The Hippocampus as a Cognitive Map. Oxford University Press. 1978.

O'Keefe, J. and Recce, M. L. Phase relationship between hippocampal place units and the EEG theta rhythm. Hippocampus 3: 317-30, 1993.

Olypher, A. V. Gamma oscillations by synaptic inhibition in a homogeneous medium model of hippocampal interneurons. Biosystems 48: 165-9, 1998.

Pare, D., deCurtis, M., and Llinas, R. Role of the hippocampal-entorhinal loop in temporal lobe epilepsy: extra- and intracellular study in the isolated guinea pig brain in vitro. J Neurosci 12: 1867-81, 1992.

Pare, D. and Llinas, R. Intracellular study of direct entorhinal inputs to field CA1 in the isolated guinea pig brain in vitro. Hippocampus 5: 115-9, 1995.

Pennartz, C. M., Lee, E., Verheul, J., Lipa, P., Barnes, C. A., and McNaughton, B. L. The ventral striatum in off-line processing: ensemble reactivation during sleep and modulation by hippocampal ripples. J Neurosci 24: 6446-56, 2004.

Penttonen, M. and Buzsaki, G. Natural logarithmic relationship between brain oscillators. Thal Relat Syst 2: 145-52, 2003.

Penttonen, M., Kamondi, A., Acsady, L., and Buzsaki, G. Gamma frequency oscillation in the hippocampus of the rat: intracellular analysis in vivo. Eur J Neurosci 10: 718-28, 1998.

Penttonen, M., Nurminen, N., Miettinen, R., Sirvio, J., Henze, D. A., Csicsvari, J., and Buzsaki, G. Ultra-slow oscillation (0.025 Hz) triggers hippocampal afterdischarges in Wistar rats. Neuroscience 94: 735-43, 1999.

Phillips, W. A. and Singer, W. In search of common foundations for cortical computation [In Process Citation]. Behav Brain Sci 20: 657-83, discussion 683-722, 1997.

Pinto, D. J., Jones, S. R., Kaper, T. J., and Kopell, N. Analysis of state-dependent transitions in frequency and long-distance coordination in a model oscillatory cortical circuit. J Comput Neurosci 15: 283-98, 2003.

Scoville, W. B. and Milner, B. Loss of recent memory after bilateral hippocampal lesions. J Neurochem 20: 11-21, 1957.

Sirota, A., Csicsvari, J., Buhl, D., and Buzsaki, G. Communication between neocortex and hippocampus during sleep in rodents. Proc Natl Acad Sci USA 100: 2065-9, 2003.

Skaggs, W. E., McNaughton, B. L., Wilson, M. A., and Barnes, C. A. Theta phase precession in hippocampal neuronal populations and the compression of temporal sequences. Hippocampus 6: 149-72, 1996.

Soltesz, I. and Deschenes, M. Low- and high-frequency membrane potential oscillations during theta activity in CA1 and CA3 pyramidal neurons of the rat hippocampus under ketamine-xylazine anesthesia. J Neurophysiol 70: 97-116, 1993.

Somjen, G. G., Aitken, P. G., Giacchino, J. L., and McNamara, J. O. Sustained potential shifts and paroxysmal discharges in hippocampal formation. J Neurophysiol 53: 1079-97, 1985.

Somogyi, P. and Klausberger T. Defined types of cortical interneurone structure space and spike timing in the hippocampus. J Physiol 562: 9-26, 2005.

Squire, L. R. and Zola-Morgan, S. The medial temporal lobe memory system. Science 253: 1380-86, 1990.

Staley, K. J., Bains, J. S., Yee, A., Hellier, J., and Longacher, J. M. Statsitical model relating CA3 burst probability to recovery from burst-induced depression at recurrent collateral synapses. J Neurophysiol 86: 2736-47, 2001.

Steriade, M. Corticothalamic networks, oscillations, and plasticity. Adv Neurol 77: 105-34, 1998.

Steriade, M. Impact of network activities on neuronal properties in corticothalamic systems. J Neurophysiol 86: 1-39, 2001.

Steriade, M. and Contreras, D. Spike-wave complexes and fast components of cortically generated seizures. I. Role of neocortex and thalamus. J Neurophysiol 80: 1439-55, 1998.

Steriade, M., McCormick, D. A., and Sejnowski, T. J. Thalamocortical oscillations in the sleeping and aroused brain. Science 262: 679-85, 1993.

Stewart, M. and Fox, S. E. Do septal neurons pace the hippocampal theta rhythm? Trends Neurosci 13: 163-8, 1990.

Swanson , L. W. The anatomical organization of septo-hippocampal projections. Ciba Found. Symp. 58: 25-48, 1977.

Timofeev, I., Grenier, F., and Steriade, M. Spike-wave complexes and fast components of cortically generated seizures. IV. Paroxysmal fast runs in cortical and thalamic neurons. J Neurophysiol 80: 1495-513, 1998.

Timofeev, I. and Steriade, M. Fast (mainly 30-100 Hz) oscillations in the cat cerebellothalamic pathway and their synchronization with cortical potentials. J Physiol (Lond) 504: 153-68, 1997.

Traub, R. D., Dudek, F. E., Snow, R. W., and Knowles, W. D. Computer simulations indicate that electrical field effects contribute to the shape of the epileptiform field potential. Neuroscience 15: 947-58, 1985.

Traub, R. D., Jefferys, J. G. R., and Whittington, M. A. Fast Oscillations in Cortical Circuits. MIT Press. 1999a.

Traub, R. D., Spruston, N., Soltesz, I., Konnerth, A., Whittington, M. A., and Jefferys, G. R. Gamma-frequency oscillations: a neuronal population phenomenon, regulated by synaptic and intrinsic cellular processes, and inducing synaptic plasticity. Prog Neurobiol 55: 563-75, 1998.

Traub, R. D., Whittington, M. A., Buhl, E. H., Jefferys, J. G., and Faulkner, H. J. On the mechanism of the gamma --> beta frequency shift in neuronal oscillations induced in rat hippocampal slices by tetanic stimulation. J Neurosci 19: 1088-105, 1999b.

Traub, R. D., Whittington, M. A., Colling, S. B., Buzsaki, G., and Jefferys, J. G. Analysis of gamma rhythms in the rat hippocampus in vitro and in vivo. J Physiol 493: 471-84, 1996.

Tsodyks, M. V., Skaggs, W. E., Sejnowski, T. J., and McNaughton, B. L. Population dynamics and theta rhythm phase precession of hippocampal place cell firing: a spiking neuron model. Hippocampus 6: 271-80, 1996.

Vanderwolf, C. H. Hippocampal electrical activity and voluntary movement in the rat. Electroencephalogr Clin Neurophysiol 26: 407-18, 1969.

Varga, V., Sik, A., Freund, T. F., and Kocsis, B. GABA(B) receptors in the median raphe nucleus: distribution and role in the serotonergic control of hippocampal activity. Neuroscience 109: 119-32, 2002.

Volgushev, M., Chistiakova, M., and Singer, W. Modification of discharge patterns of neocortical neurons by induced oscillations of the membrane potential. Neuroscience 83: 15-25, 1998.

Wadman, W. J., Juta, A. J., Kamphuis, W., and Somjen, G. G. Current source density of sustained potential

shifts associated with electrographic seizures and with spreading depression in rat hippocampus. Brain Res 570: 85-91, 1992.

Wallenstein, G. V. and Hasselmo, M. E. GABAergic modulation of hippocampal population activity: sequence learning, place field development, and the phase precession effect. J Neurophysiol 78: 393-408, 1997.

Wang, X. J. and Buzsaki, G. Gamma oscillation by synaptic inhibition in a hippocampal interneuronal network model. J Neurosci 16: 6402-13, 1996a.

Whittington, M. A., Doheny, H. C., Traub, R. D., LeBeau, F. E., and Buhl, E. H. Differential expression of synaptic and nonsynaptic mechanisms underlying stimulus-induced gamma oscillations in vitro. J Neurosci 21: 1727-38, 2001.

Whittington, M. A., Stanford, I. M., Colling, S. B., Jefferys, J. G., and Traub, R. D. Spatiotemporal patterns of gamma frequency oscillations tetanically induced in the rat hippocampal slice. J Physiol (Lond) 502: 591-607, 1997.

Whittington, M. A., Traub, R. D., and Jefferys, J. G. Synchronized oscillations in interneuron networks driven by metabotropic glutamate receptor activation. Nature 373: 612-5, 1995.

Whittington, M. A., Traub, R. D., Kopell, N., Ermentrout, B., and Buhl, E. H. Inhibition-based rhythms: experimental and mathematical observations on network dynamics. Int J Psychophysiol 38: 315-36, 2000.

Wong, R. K., Miles, R., and Traub, R. D. Local circuit interactions in synchronization of cortical neurones. J Exp Biol 112: 169-78, 1984.

Wu, K. and Leung, L. S. Increased dendritic excitability in hippocampal ca1 in vivo in the kainic acid model of temporal lobe epilepsy: a study using current source density analysis. Neuroscience 116: 599-616, 2003.

Ylinen, A., Bragin, A., Nadasdy, Z., Jando, G., Szabo, I., Sik, A., and Buzsaki, G. Sharp wave-associated high-frequency oscillation (200 Hz) in the intact hippocampus: network and intracellular mechanisms. J Neurosci 15: 30-46, 1995a.

Ylinen, A., Soltesz, I., Bragin, A., Penttonen, M., Sik, A., and Buzsaki, G. Intracellular correlates of hippocampal theta rhythm in identified pyramidal cells, granule cells, and basket cells. Hippocampus 5: 78-90, 1995b.

Yun, S. H., Mook-Jung, I., and Jung, M. W. Variation in effective stimulus patterns for induction of long-term potentiation across different layers of rat entorhinal cortex. J Neurosci 22: 1-5, 2002.

Zador, A., Koch, C., and Brown, T. H. Biophysical model of a Hebbian synapse. Proc Natl Acad Sci USA 87: 6718-22, 1990.

Zugaro, M. B., Monconduit, L., and Buzsaki, G. Spike phase precession persists after transient intrahippocampal perturbation. Nat Neurosci 8: 67-71, 2005.

Kuopio University Publications G. - A.I.Virtanen Institute

G 22. Törönen, Petri. Analysis of gene expression data using clustering and functional classification.
2004. 65 p. Acad. Diss.

G 23. Nurmi, Antti. The role of nuclear factor kappa-B in models of adult and neonatal cerebral ischemia: the effects of pyrrolidine dithiocarbamate.
2004. 144 p. Acad. Diss.

G 24. Kankkonen, Hanna. Gene therapy in the treatment of familial hypercholesterolemia: evaluation and development of viral vectors and gene transfer techniques.
2004. 107 p. Acad. Diss.

G 25. Rutanen, Juha. Vascular endothelial growth factors in atherosclerosis and gene therapy for restenosis and myocardial ischemia.
2005. 81 p. Acad. Diss.

G 26. Koponen, Eija. Increased BDNF signaling in adult brain : an experimental study using transgenic mice overexpressing the functional trkB receptor.
2005. 96 p. Acad. Diss.

G 27. Narkilahti, Susanna. Expression and activation of caspases in the brain during epileptogenesi: experimental study in rat.
2005. 77 p. Acad. Diss.

G 28. Magga, Johanna. G protein mediated calcium signaling in the regulation of synaptic transmission.
2005. 78 p. Acad. Diss.

G 29. Bhardwaj, Shalini. Adenovirus mediated growth factor gene transfer to periadventitial space: effects on angiogenesis and intimal hyperplasia.
2005. 75 p. Acad. Diss.

G 30. Keinänen, Riitta et al. (Eds.). The tenth annual post-graduate symposium of the A. I. Virtanen Institute Graduate School: AIVI Winter School 2005.
2005. 64 p. Abstracts.

G 31. Päivärinta, Maija. Phosphatidylinositol 3-kinase and type 2 diabetes: catalytic subunit p110ß as a candidate gene for type 2 diabetes and in vitro modelling of the insulin signalling pathway.
2005. 83 p. Acad. Diss.

G 32. Turunen, Päivi. Gene therapy of restenosis and vein graft disease studies with single genes and gene combinations.
2005. 78 p. Acad. Diss.

G 33. Puhakka, Hanna. Gene therapy for vascular thickening.
2005. 82 p. Acad. Diss.

G 34. Cao, Jiong. The regulation and role of stress-activated protein kinases (p38 and JNK) in neuronal cell death.
2005. 79 p. Acad. Diss.

G 35. Hakkarainen, Tanja. Enhancement of cancer gene therapy with modified viral vectors and fusion genes.
2005. 63 p. Acad. Diss.

G 36. Valonen, Piia. A multimodal NMR study of apoptosis induced by HSV-tk gene therapy in a rat experimental glioma model.
2005. 87 p. Acad. Diss.